based on PRD84,2011; 1108.4344 [hep-ph]; 1109.2718 [hep-ph]

Pion-photon transition form factor in light-cone sum rules: theoretical results, expectations, and a global-data fit.

S. Mikhailov[1], A. Bakulev[1], A. Pimikov[1], and N. Stefanis[2]

[1] Bogoliubov Laboratory of Theoretical Physics, Dubna, Russia
[2] Ruhr-Universität Bochum, Germany

QFTHEP'2011,
Sochi, September 25th – October 1st

September 25, 2011

- **electron $e_{\rm tag}$ is detected and identified**
- **meson π^0 is detected and fully reconstructed**

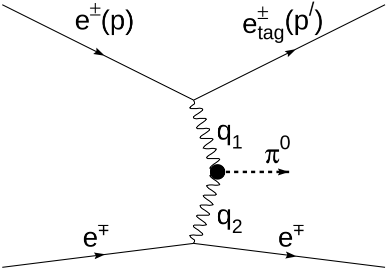

Why it is interesting for QCD?

- The measurements of $\gamma^*\gamma \to \pi^0$ form factor in **CELLO91**, **CLEO98**, and especially **BaBar09** experiments have **the best accuracy** among others exclusive hard processes
- We have significant theoretical advances in **QCD** here: **high order NNLO$_\beta$ contribution** to the hard part of the form factor; also the contributions from twist-4 and **higher order inverse power corrections a'la twist-6**
- The data of **BaBar09** Collab. for this process creates **the pion puzzle** – **the challenge to collinear QCD**

BaBar data [June 2009] on pion-photon transition form factor **grows like $\sqrt{Q}$, while behavior like $Q^2/(Q^2+\Lambda^2)$ was expected**

[B. Aubert, Phys. Rev. D 80, 052002 (2009)]: [arXiv:1101.1142]:

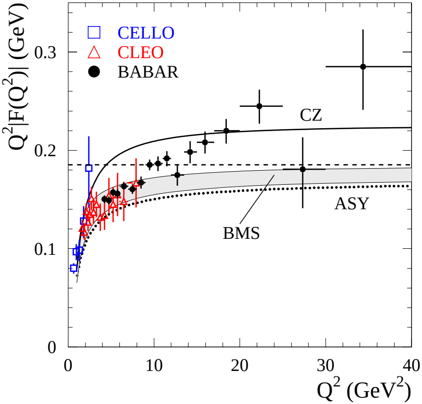

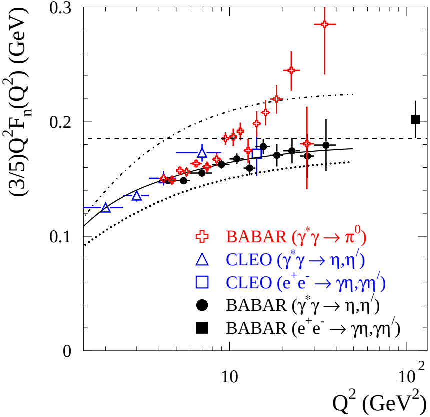

These authors claimed (2011):

"If the experiment is correct, many theoretical predictions should be revised..."

Current status of the the pion puzzle [September 2011, PhiPsi'11]

BaBar Collaboration reports:
"Transition form factors and two-photon physics from BaBar"

- **They confirmed 'status quo':**
  "An unexpected Q^2 dependence of the $\gamma^*\gamma \to \pi^0$ form factor is observed"
- **"The next measurement of the pion-photon transition form factor confirming or refuting BABAR result will be performed at Super-B factories in 5-10 years."**

Belle Collaboration reports:
"Recent results on two-photon physics at Belle "

- **No expected news concerning the $\gamma^*\gamma \to \pi^0$ form factor**

Plan – to present the Theoretical Basis of the consideration

1. **$\gamma^*(q_1)\gamma^*(q_2) \to \pi^0(p)$, factorization, structure of $F^{\gamma^*\gamma^*\pi}$**
   - Introduction to collinear factorization
   - Hard-scattering amplitudes in NLO, T_1, NNLO, T_2, meson Distribution Amplitudes (DA) φ

2. **Pion Distribution Amplitudes φ_π**
   - Nonlocal condensates and **BMS bunch** of pion DAs

3. **Light Cone Sum Rules (LCSR) for $\gamma^*\gamma(q_2^2 \simeq 0)$**
   - Why Light Cone Sum Rules (LCSR)? Dispersion relations for $\mathbf{F}^{\gamma^*\gamma\pi}$
   - NLO Spectral density ρ_1
   - Direct predictions of $F^{\gamma^*\gamma\pi}_{\text{LCSR}}$ vs CELLO and CLEO data

4. **High order corrections**
   - β_0-part of NNLO spectral density ρ_2 and "twist 6" contribution
   - The result of high order contributions to $\mathbf{F}^{\gamma^*\gamma\pi}$

Plan – to present the fit of experimental data

1. **Direct predictions of $F^{\gamma^*\gamma\pi}_{\mathbf{LCSR}}$ vs CELLO, CLEO and BaBar data**

2. **Inverse Problem: fitting pion DA from experimental data**
   - **3D** analysis of pion DA
   - **2D** analysis of pion DA

3. **2D Constraints and Lattice QCD**

4. **Conclusions**

$$\gamma^*(q_1)\gamma^*(q_2) \longrightarrow \pi^0(p),$$

collinear factorization, and structure of $F^{\gamma^*\gamma^*\pi}$

$\gamma^*(q_1)\gamma^*(q_2) \to \pi^0(P)$ in pQCD

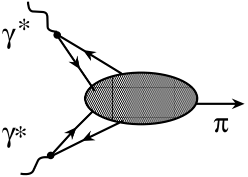

$$\int d^4 z e^{-iq_1 \cdot z} \langle \pi^0(P) \mid T\{j_\mu(z) j_\nu(0)\} \mid 0\rangle =$$

$$i\epsilon_{\mu\nu\alpha\beta} q_1^\alpha q_2^\beta \cdot \boldsymbol{F^{\gamma^*\gamma^*\pi}(Q^2, q^2)}\,,$$

$$-\boldsymbol{q_1^2} = \boldsymbol{Q^2} > \boldsymbol{0}, \quad -\boldsymbol{q_2^2} = \boldsymbol{q^2} \geq \boldsymbol{0}$$

Collinear factorization at $Q^2, q^2 \gg$ (hadron scale$\sim m_\rho)^2$

$$F^{\gamma^*\gamma^*\pi}(Q^2, q^2) = \boldsymbol{T(Q^2, q^2, \mu_F^2; x)} \otimes \boldsymbol{\varphi_\pi^{(2)}(x; \mu_F^2)} + O(\frac{1}{Q^4})$$

$\boldsymbol{\mu_F^2}$ – boundary between **hard scale** and **hadronic one**.

For leading twist 2 and at parton level

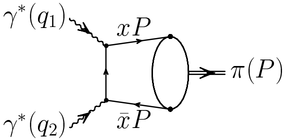

$$F^{\gamma^*\gamma^*\pi}(Q^2, q^2) = \frac{\sqrt{2}}{3} f_\pi \int_0^1 dx \, \frac{\boldsymbol{1}}{\boldsymbol{Q^2 x + q^2 \bar{x}}} \; \boldsymbol{\varphi_\pi^{(2)}(x; \mu_F^2)}$$

$$Q^2 F^{\gamma^*\gamma\pi}(Q^2, q^2 \to 0) = \frac{\sqrt{2}}{3} f_\pi \int_0^1 \frac{\boldsymbol{dx}}{\boldsymbol{x}} \boldsymbol{\varphi_\pi^{(2)}(x)}$$

$$\equiv \frac{\sqrt{2}}{3} f_\pi \langle \boldsymbol{x^{-1}} \rangle_{\boldsymbol{\pi}}$$

Distribution amplitudes in exclusive reactions

$$< 0|\bar{q}(z)\gamma_\mu\gamma_5 E(z,0)q(0)|\pi(P) > \Big|_{z^2=0} = iP_\mu f_\pi \int dx e^{ix(zp)} \boldsymbol{\varphi_\pi^{(2)}(x,\mu_F^2)}$$

$$E(z,0) = P\exp(ig\int_0^z A_\mu(\tau)d\tau^\mu)$$

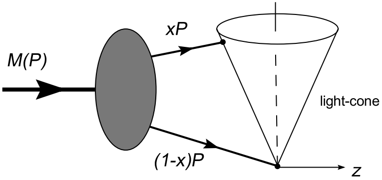

Distribution amplitudes are **nonperturbative** quantities to be derived from

- **QCD SR [CZ 1984],**
  NLC QCD SR [M&Radyushkin1988-91,Bakulev&M&Stefanis1998,2001–04]
- **instanton-vacuum approaches,**
  [Dorokhov *et al.* 2000; Polyakov *et al.* **1998, 2009]**
- **Lattice QCD, [Braun *et al.* 2006; Arthur *et al.* 2011]**
- **from experimental data [Schmedding&Yakovlev 2000, BMS 2003–2006]**

But DA evolves with μ_F^2 according to ERBL equation in pQCD

NLO evolution DA with scale μ^2

$\varphi(x;\mu^2) \longrightarrow \varphi(x;Q^2)$ evolves according to **NLO ERBL [79-80]** equation:

$$\mu^2 \frac{d}{d\mu^2}\varphi(x;\mu^2) \quad = \quad \Big(a_s\ V_+^{(0)}(x,y) + a_s^2\ V_+^{(1)}(x,y)\Big) \otimes \varphi(y;\mu^2)$$

$$\Big(V^{(0)} = V^a + V^b\Big) \otimes \psi_n = 2C_{\rm F}\, v(n) \cdot \psi_n$$

Eigenfunctions: $\psi_n(x) = 6x\bar{x}\ C_n^{(3/2)}(x-\bar{x})$ – **Gegenbauer harmonics**

Eigen modes: $v(n)$

$$\varphi_\pi^{(2)}(x;\mu^2) = \psi_0(x) + a_2(\mu^2)\ \psi_2(x) + a_4(\mu^2)\ \psi_4(x) + a_6(\mu^2)\ \psi_6(x) + \ldots$$

NLO and NNLO amplitudes.

Collinear factorization is Theorem **[Efremov&Radyushkin 1978]**

$$F^{\gamma^*\gamma^*\pi} \sim \left(T_0(Q^2,q^2;x) + a_s^1\, T_1(Q^2,q^2;\mu_F^2;x) + a_s^2\, T_2(Q^2,q^2;\mu_F^2;\mu_R^2;x) + \ldots\right) \otimes \boldsymbol{\varphi_\pi^{(2)}(x;\mu_F^2)} - \boldsymbol{\delta^2_{tw4}(\mu_F^2)} \cdot T_0^2(Q^2,q^2;x) \otimes \boldsymbol{\varphi_\pi^{(4)}(x)}$$

T_i — **calculable in pQCD,** $a_s(\mu_R^2) = \alpha_s/(4\pi)$. Usually sets $\mu_R^2 = \mu_F^2$ **to simplify** and $\mu_F^2 = \langle Q^2 \rangle$ **to minimize** rad. corrections.
$\boldsymbol{\delta^2_{tw4} = (0.19 \pm 0.02)}$ **GeV**^{2} – twist-4 scale parameter.

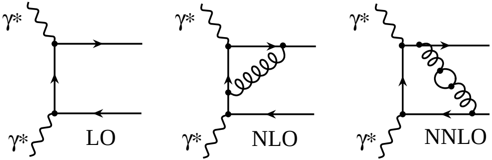

LO: $$T_0(Q^2,q^2;x) = \frac{1}{x\,Q^2 + \bar{x}\,q^2}$$

NLO hard amplitudes

NLO (last editions):

[Bakulev&MS&Stefanis(2003)], [Melić&Müller&Passek(2003)]

$$T_1\left(x; Q^2, q^2\right) \otimes \varphi(x) = T_0(Q^2, q^2; y) \otimes \left\{C_{\mathrm{F}} \mathcal{T}^{(1)}(y,x) + \mathbf{L}(\boldsymbol{y}) \cdot \boldsymbol{V}^{(0)}(y,x)\right\} \otimes \boldsymbol{\varphi}(\boldsymbol{x}; \boldsymbol{\mu}_F^2)$$

$$\mathcal{T}^{(1)} = \left[-3\boldsymbol{V}^{b} + \boldsymbol{g}\right](x,y)_{+} - 3\delta(x-y), \qquad \mathbf{L}(\boldsymbol{y}) \equiv \ln\left[\left(Q^2 y + q^2 \bar{y}\right)/\mu_{\mathrm{F}}^2\right]$$

$$\boldsymbol{g}(x,y) = -2\frac{\theta(y>x)}{y-x}\ln(1-x/y) + (x \to \bar{x},\ y \to \bar{y})$$

NNLO amplitude and coefficient functions

β_0-part of NNLO: $\boldsymbol{T}_2 \otimes \varphi \longrightarrow \beta_0 \cdot \boldsymbol{T}_\beta \otimes \varphi$, at $\mu_{\rm R}^2 = \mu_{\rm F}^2$
[Melić&Müller&Passek(2003)]

$$a_s^2 \beta_0 T_\beta \otimes \varphi = a_s^2 \beta_0 T_0 \otimes \Big\{ C_{\rm F} \mathcal{T}_\beta^{(2)} - C_{\rm F} \mathbf{L}(y) \cdot \mathcal{T}^{(1)} + \mathbf{L}(y) \cdot \left(V_\beta^{(1)}\right)_+ - \frac{1}{2} \mathbf{L}^2(y) \cdot V_+^{(0)} \Big\} \otimes \varphi \,.$$

The origins of these terms:
$\sim \mathbf{L}(y)\ \mathcal{T}^{(1)}$ – 1-loop RG-evolution
$\sim \mathbf{L}^2(y)\ V_+^{(0)}$ – 1-loop ERBL-evolution together with RG-a_s one, while
$\sim \mathbf{L}(y)\ \left(V_\beta^{(1)}\right)_+$ – as the β_0-part of 2-loop ERBL kernel;
$\sim \mathcal{T}_\beta^{(2)}$ – the β_0-part of the coefficient function $\mathcal{T}^{(2)}$
These terms together form the exponential ERBL-solution:

$$\exp\left\{ \int^{\mathbf{L}} V(a_s(L))dL \right\}$$

$\mathcal{T}_\beta^{(2)}$ – the coefficient function – **original, the most cumbersome part**
This contribution gives the sign and size of NNLO effect following to BLM prescription

Pion Distribution Amplitude in QCD SR with Nonlocal condensates

Pion distribution amplitude in NLC QCD SRs

$$\varphi_\pi^{(2)}(x;\mu_{\rm F}^2) = \psi_0(x) + a_2(\mu_{\rm F}^2)\ \psi_2(x) + a_4(\mu_{\rm F}^2)\ \psi_4(x) + \ldots$$

$\varphi_\pi^{(2)} \Leftrightarrow \{a_n\}$; partial waves: $\psi_n(x) = 6x\bar{x}\ C_n^{(3/2)}(x-\bar{x})$ (Gegenbauer harmonics)

BMS estimates for a_2, a_4 **[PLB 508 (2001) 279]**

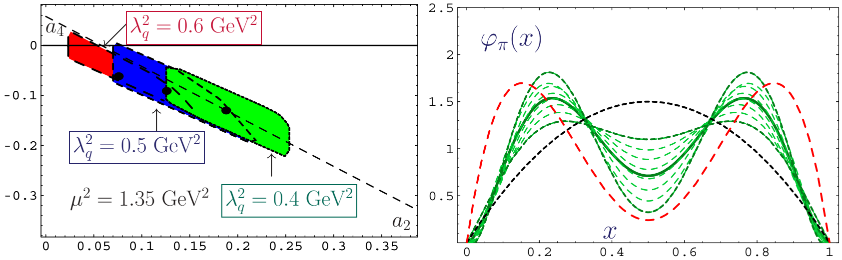

- **Green rectangle** forms **BMS "bunch"** of DAs, $\psi_0 + a_2\psi_2 + a_4\psi_4$ (Best-fit values—thick green line RHS: $a_2 = 0.2$, $a_4 = -0.14$)
- ψ_0 – Asymptotic (As) DA (dotted line: $a_{2n} = 0$)
- **Chernyak-Zhitnitsky (CZ)** DA, $\psi_0 + a_2\psi_2$ (red dashed line RHS: $a_2(\mu^2 = 1\ \mathrm{GeV}^2) = 0.56$, $a_4 = 0$)
- **"Flat distribution"** corresponds to $a_n \sim 1/n$

Light Cone Sum Rules (LCSR)

Why Light Cone Sum Rules (LCSR)?

The experimental conditions prefer $q^2 \longrightarrow 0$

For $Q^2 \gg m_\rho^2, \;\; q^2 \ll m_\rho^2$ pQCD factorization valid only in leading–twist approximation; hence, higher twists become important. Reason: if $q^2 \longrightarrow 0$, one needs to take into account interaction of real photon at long distances of order of $O(1/\sqrt{q^2})$

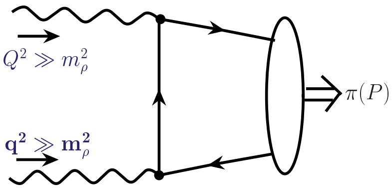

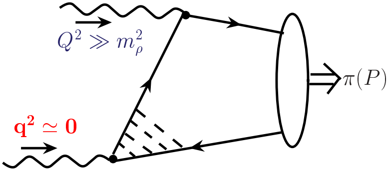

pQCD is OK **photon behaves like a hadron**

LCSR effectively accounts for long-distance effects of real photon using **[Khodjamirian, EJPC (1999)]**:

- **dispersion relation in variable q^2**
- **quark-hadron duality in vector channel.**

Dispersion relation for $F^{\gamma^*\gamma\pi}$

The main further goal – spectral density ρ

$$F^{\gamma^*\gamma^*\pi}(Q^2,q^2) = \int\limits_0^\infty ds\ \frac{\rho^{\mathrm{ph}}(Q^2,s)}{s+q^2}$$

$$\rho^{\mathrm{ph}} = \theta(s_0-s)\ \rho^{\mathrm{phen}}(Q^2,s) + \theta(s-s_0)\ \rho^{\mathrm{PT}}(Q^2,s)$$

$$\begin{aligned}\rho^{\mathrm{PT}}(Q^2,s) &= \frac{\mathbf{Im}}{\pi}\Big[F^{\gamma^*\gamma^*\pi}(Q^2,-s-i\varepsilon)\Big]\\ \rho^{\mathrm{phen}}(Q^2,s) &= \sqrt{2}f_\rho F^{\gamma^* V\pi}(Q^2)\cdot\delta(s-m_V^2)\Big|_{V=\rho,\omega}\end{aligned}$$

using quark-hadron duality in vector channel for $F^{\gamma^* V\pi}$ **[Khodjamirian 1999]:**

$$\begin{aligned}F^{\gamma\gamma^*\pi}(Q^2,q^2\to 0) &= \frac{1}{\pi}\int_{s_0}^{\infty}\frac{\mathrm{Im}F^{\gamma^*\gamma^*\pi}(Q^2,-s)}{s}\,ds, \quad \text{"H–part"}\\ &+\ \frac{1}{\pi}\int_0^{s_0}\frac{\mathrm{Im}F^{\gamma^*\gamma^*\pi}(Q^2,-s)}{m_\rho^2}\,e^{(m_\rho^2-s)/M^2}\,ds, \quad \text{"V–part"}\end{aligned}$$

$s_0 \simeq 1.5$ GeV^2 – effective threshold in vector channel,

M^2–Borel parameter depends on Q^2, $M^2 = 0.7/\langle x\rangle_{Q^2} = 0.7 - 0.9$ GeV^2.

NLO Spectral density $\rho^{(1)}$

$$\rho^{(1)}(Q^2,s) = \frac{\mathbf{Im}}{\pi}\left[(T_1 \otimes \varphi_\pi)(Q^2,-s-i\varepsilon)\right]\,,\; s \geq 0$$

$\rho_n^{(1)}(x,\mu_F^2)$ for Gegenbauer harmonic ψ_n, $\boxed{x = Q^2/(s+Q^2)}$

The general case [M&Stefanis(2009)], partly corrected in [Agaev et al (2011)]:

$$\begin{aligned}\bar{\rho}_n^{(1)}\left(x;\mu_{\mathrm{F}}^2\right) \quad = \quad & C_{\mathrm{F}}\left\{-3\left[1+v^b(n)\right]+\frac{\pi^2}{3}-\ln^2\left(\frac{\bar{x}}{x}\right)+2v(n)\ln\left(\frac{\bar{x}}{x}\frac{Q^2}{\mu_{\mathrm{F}}^2}\right)\right\}\psi_n(x) \\ & -C_{\mathrm{F}}2\left[\sum_{l=0,2,\ldots}^{n} G_{nl}\psi_l(x) + v(n)\cdot\left(\sum_{m=1,2,\ldots}^{n} b_{nm}\psi_m(x) - 3\bar{x}\right)\right]\end{aligned}$$

G_{nl} (originates from g), b_{nl} – calculable triangular matrices

The partial case $\bar{\rho}_0^{(1)}$ [Schmedding&Yakovlev (2000)]:

$$\bar{\rho}_0^{(1)}(x) = C_{\mathrm{F}}\left[-5+\frac{\pi^2}{3}-\ln^2\left(\frac{\bar{x}}{x}\right)\right]\psi_0(x)$$

Conclusion: The NLO spectral density and $F^{\gamma\gamma^*\pi}$ are obtained for Any numbers of Gegenbauer harmonics

NLO LCSR vs. CELLO (♦) & CLEO (▲) data

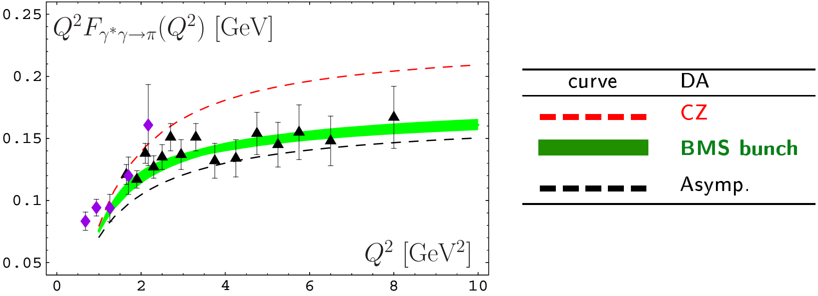

Radiative corrections contribute up to -17% at low/moderate Q^2

- **BMS "bunch"** describes rather well all data above $Q^2 \gtrsim 1.5$ GeV^2 at $\chi^2_{\text{ndf}} = 0.6 \div 1$;
- Low-Q^2 CELLO data **excludes Asy DA**
- high-Q^2 CLEO data **excludes CZ DA**

These latter items confirm the first observations by **[Kroll et al (1996)]**

High order corrections:

NNLO$_{\beta_0}$ and twist 6 contributions to $Q^2 F^{\gamma^*\gamma\pi}$

NNLO$_{\beta_0}$ Spectral density [M&Stefanis(2009)]

$$\rho^{(2)}(Q^2,s) = \frac{\mathbf{Im}}{\pi}\left[(T_2 \otimes \varphi_\pi)(Q^2, -s - i\varepsilon)\right]\,,\ s \geq 0$$

$$\bar{\rho}_n^{(2)} \;\rightarrow\; \bar{\rho}_n^{(2\beta)}(Q^2,x) = \beta_0 C_{\rm F}\left[\bar{R}_n^{(2)}\left(x; \frac{\bar{x}}{x}\frac{Q^2}{\mu_{\rm F}^2}\right)\right],\ \boxed{x = Q^2/(s+Q^2)},\ \text{put } \boldsymbol{\mu_{\rm R}^2 = \mu_{\rm F}^2}$$

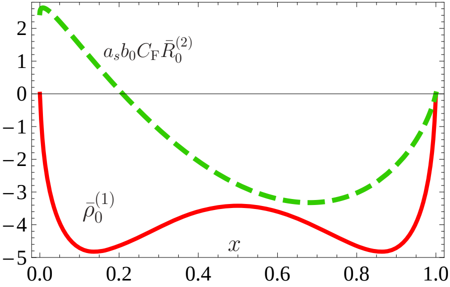

The **dashed green line** shows $a_s(\mu_{\rm F}^2)\ \bar{\rho}_0^{(2\beta)} = a_s(\mu_{\rm F}^2)\ \beta_0 C_{\rm F} \bar{R}_0^{(2)}(x, \bar{x}/x)$ at the typical CLEO scale $\langle Q^2 \rangle = \mu_{\rm F}^2 = (2.4\ \text{GeV})^2$, whereas the **solid red line** represents $\bar{\rho}_0^{(1)}(x)$

Conclusion: The NNLO$_\beta$ spectral density and $F^{\gamma\gamma^*\pi}$ are obtained for 6 numbers of Gegenbauer harmonics

Main Ingredients of Spectral Density

We denote

$$\rho(Q^2, s) = \rho^{(0)}(Q^2, s) + a_s\rho^{(1)}(Q^2, s) + a_s^2\rho^{(2)}(Q^2, s)$$

- **NLO Spectral Density — in [Mikhailov&Stefanis(2009)], partially corrected in [ABOP(2011)]:**

$$\rho^{(1)}(Q^2, s) = \frac{\mathbf{Im}}{\pi}\left[\left(T_1 \otimes \varphi_\pi\right)\left(Q^2, -s - i\varepsilon\right)\right], s \geq 0$$

Main Ingredients of Spectral Density

We denote

$$\rho(Q^2,s) = \rho^{(0)}(Q^2,s) + a_s\rho^{(1)}(Q^2,s) + a_s^2\rho^{(2)}(Q^2,s)$$

- **NLO Spectral Density — in [Mikhailov&Stefanis(2009)], partially corrected in [ABOP(2011)]:**

$$\rho^{(1)}(Q^2,s) = \frac{\mathrm{Im}}{\pi}\left[\left(T_1 \otimes \varphi_\pi\right)\left(Q^2,-s-i\varepsilon\right)\right],\, s \geq 0$$

- **NNLO$_{\beta_0}$ Spectral Density — in [M&S(2009)]**

$$\rho^{(2,\beta)}(Q^2,s) = \beta_0\frac{\mathrm{Im}}{\pi}\left[\left(T_{2\beta} \otimes \varphi_\pi\right)\left(Q^2,-s-i\varepsilon\right)\right],\ s \geq 0$$

Both $\rho^{(1)}$ and $\rho^{(2,\beta)}$ are obtained for arbitrary Gegenbauer harmonic.

Main Ingredients of Spectral Density

We denote

$$\rho(Q^2,s) = \rho^{(0)}(Q^2,s) + a_s\rho^{(1)}(Q^2,s) + a_s^2\rho^{(2)}(Q^2,s)$$

- **NLO Spectral Density — in [Mikhailov&Stefanis(2009)], partially corrected in [ABOP(2011)]:**

$$\rho^{(1)}(Q^2,s) = \frac{\mathbf{Im}}{\pi}\left[\left(T_1 \otimes \varphi_\pi\right)\left(Q^2, -s - i\varepsilon\right)\right], s \geq 0$$

- **NNLO$_{\beta_0}$ Spectral Density — in [M&S(2009)]**

$$\rho^{(2,\beta)}(Q^2,s) = \beta_0\frac{\mathbf{Im}}{\pi}\left[\left(T_{2\beta} \otimes \varphi_\pi\right)\left(Q^2, -s - i\varepsilon\right)\right],\ s \geq 0$$

  Both $\rho^{(1)}$ and $\rho^{(2,\beta)}$ are obtained for arbitrary Gegenbauer harmonic.

- **"Tw-6" contribution — in [ABOP–PRD83(2011)0540020]**

$$\rho^{\text{tw6}}(Q^2,x) = 8\pi C_F\frac{\alpha_s\langle\overline{q}q\rangle^2}{N_c f_\pi^2}\frac{x^2}{Q^6}\left[2x\ln x\overline{x} - x + 2\delta(\overline{x}) - \left[\frac{1}{1-x}\right]_+\right]$$

High order corrections result

Twist-6 and NNLO$_{\beta_0}$ contributions to the $Q^2 F^{\gamma^*\gamma\pi}(Q^2)$ with BMS-like Pion DA

They practically cancel out each other [BMPS(2011)]

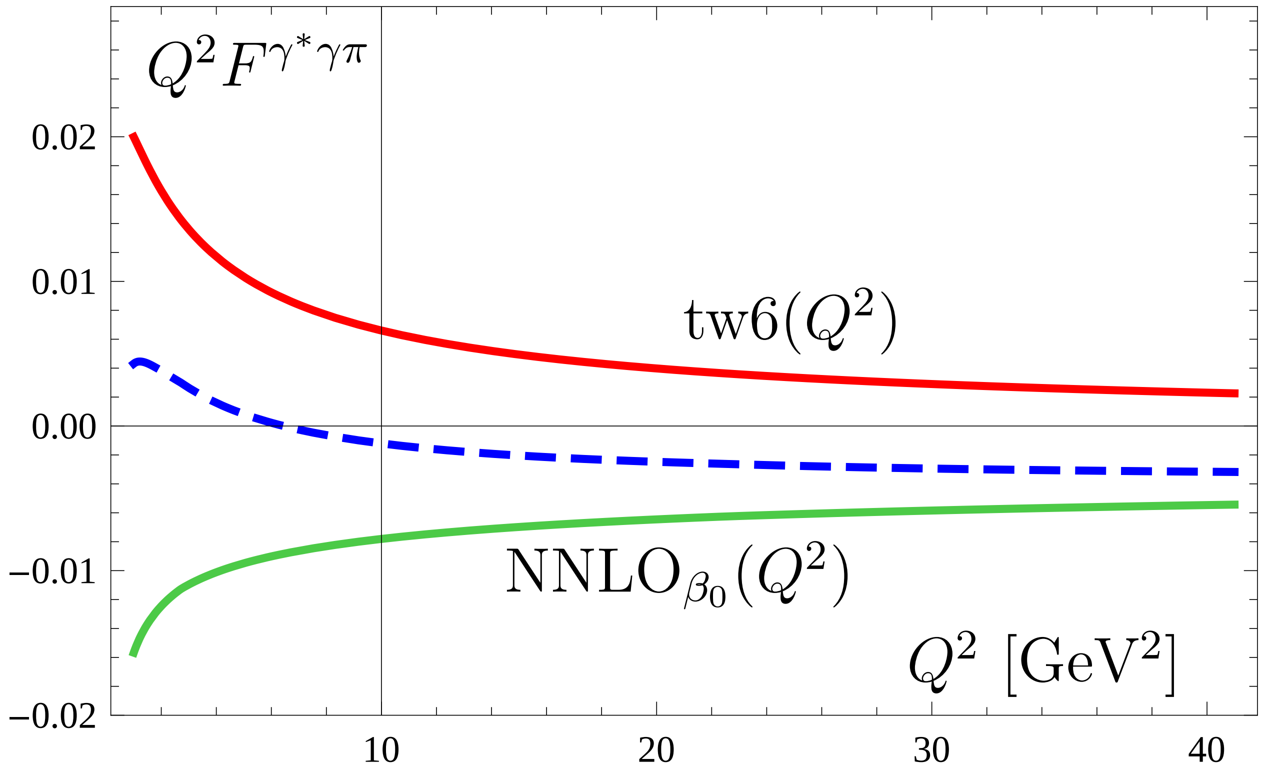

We use this residual as theoretical uncertainty of our prediction, that provides us with an additional 3%-uncertainty.

Pie chart for Pion-Photon TFF at $Q^2 = 8$ GeV^2

- **Result is dominated by Hard Part of Twist-2 LO contribution.**

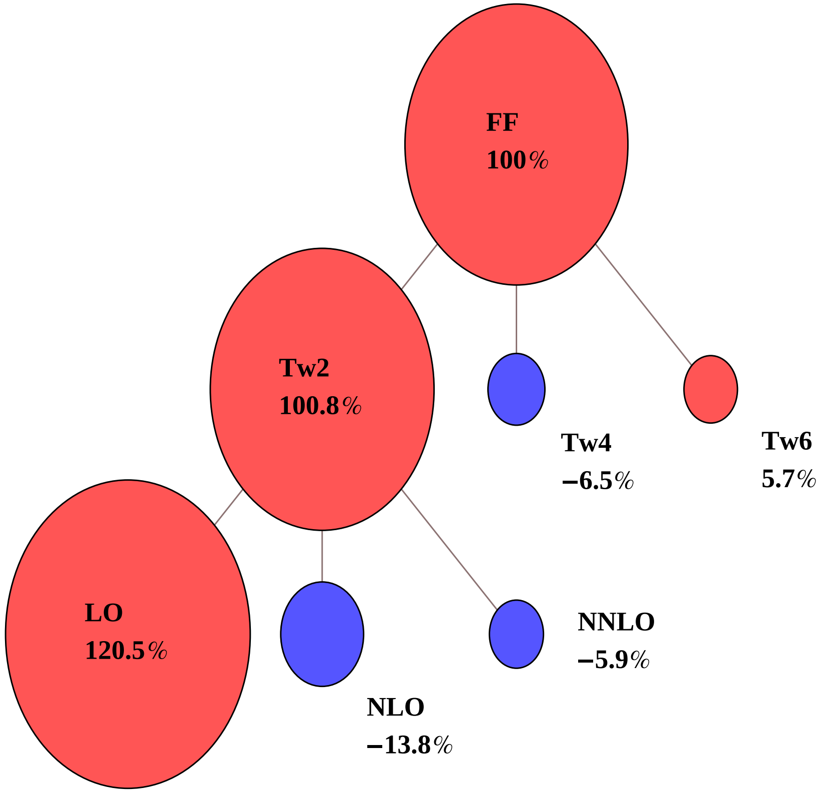

Blue = negative terms

Red = positive terms

Pie chart for Pion-Photon TFF at $Q^2 = 8\,\text{GeV}^2$

- **Result is dominated by Hard Part of Twist-2 LO contribution.**
- **Twist-6 contribution is taken into account together with NNLO$_{\beta_0}$ one — they has close absolute values and opposite signs.**

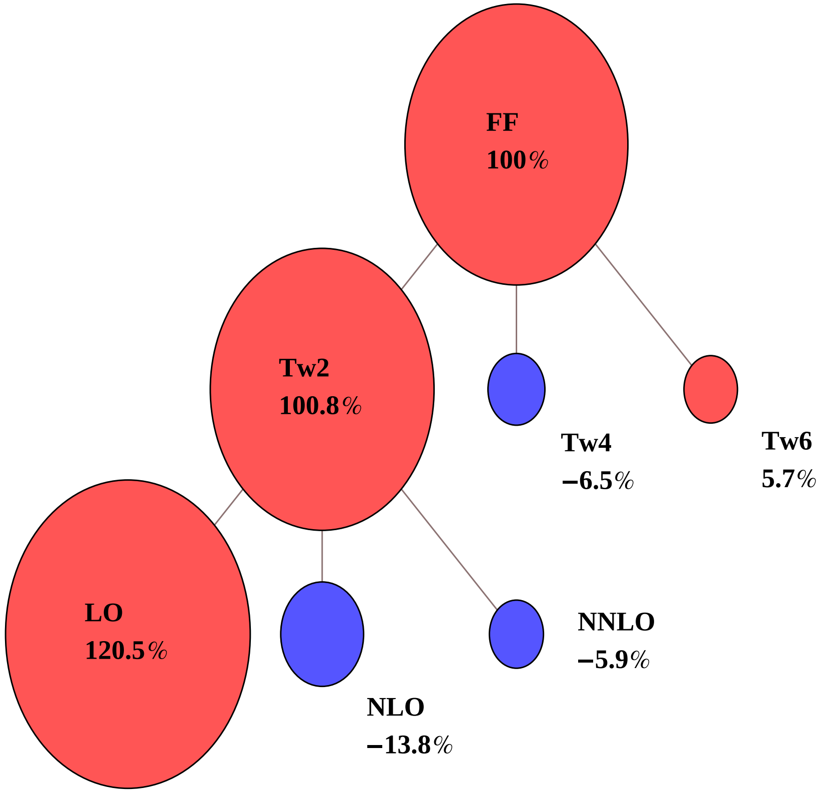

Blue = negative terms

Red = positive terms

Parameters of LCSRs

From PDG:

- $\alpha_s(m_Z^2)$
- Masses m_ρ, m_ω
- Decay Widths Γ_ρ, Γ_ω (for quasireal real γ)

From QCD SR:

- Borel parameter M^2_{LCSR}
- Vector Chan. Threshold s_0
- Twist-4 $\delta^2 \pm 20\%$
- Twist-6 ($\alpha_S\langle\bar{q}q\rangle$)

Light-Cone Sum Rules:

$$\overbrace{\text{LO} + \text{NLO} + \text{Tw-4} + (\text{NNLO}_{\beta_0} + \text{Tw-6})}$$

π-DA model

Data on FF

FF Prediction

Fitting π-DA (a_n)

Direct Problem:
LCSRs Results
for
Pion-Gamma Transition FF

Pion-gamma FF vs Experimental Data

Comparison with all data: CELLO, CLEO and BaBar

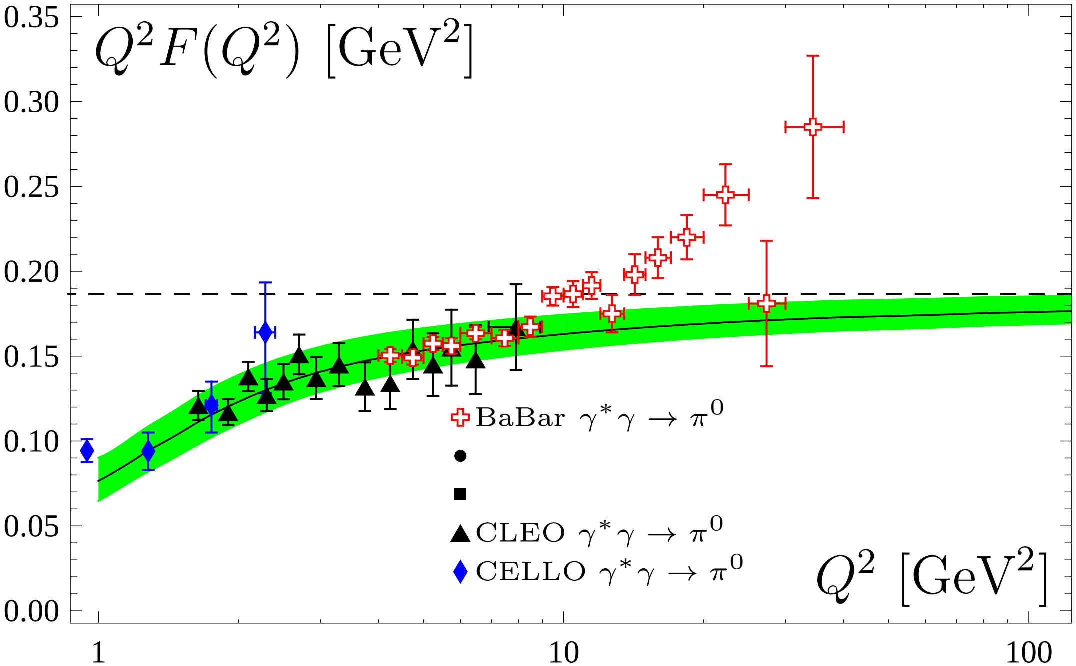

curve	DA
– – – – –	Asymp.QCD
(green band)	BMS bunch

- **BMS bunch describes very good all data for $Q^2 \leq 9$ GeV^2.**

Pion-gamma FF vs Experimental Data

Comparison with all data: CELLO, CLEO and BaBar

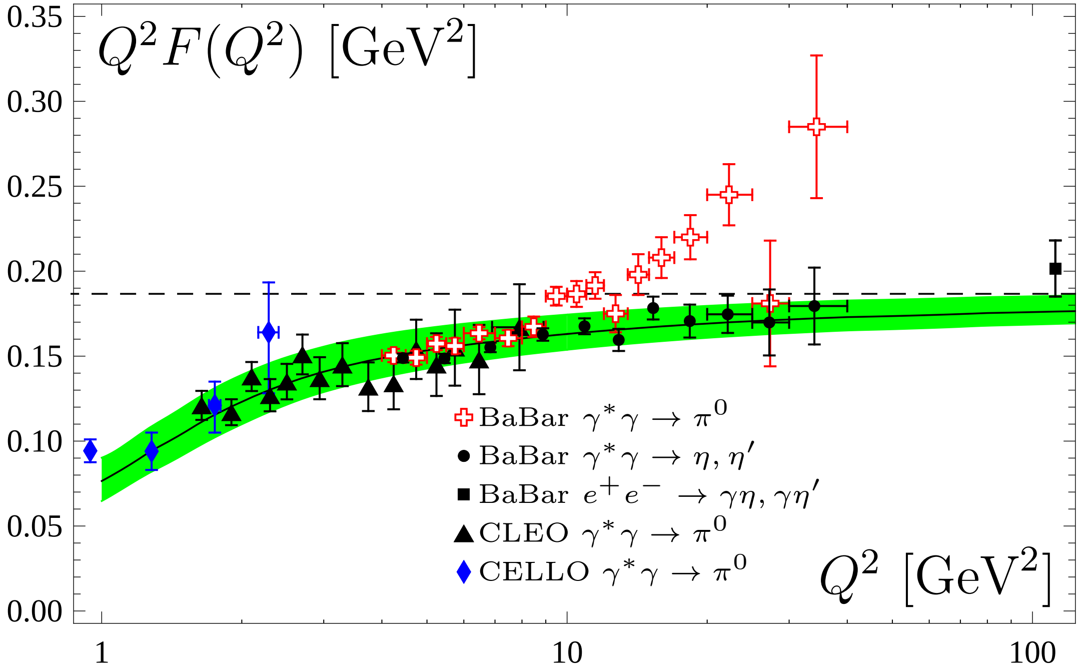

curve	DA
– – – – –	Asymp.QCD
(green band)	BMS bunch

- **BMS bunch describes very good all data for $Q^2 \leq 9$ GeV^2.**
- **Note added BaBar $\gamma^*\gamma \to \eta, \eta'$ and $e^+e^- \to \gamma\eta, \gamma\eta'$ data (1101.1142[hep-ex]): All they are inside BMS strip !**

Pion-gamma FF vs Experimental Data

Comparison with all data: CELLO, CLEO and BaBar

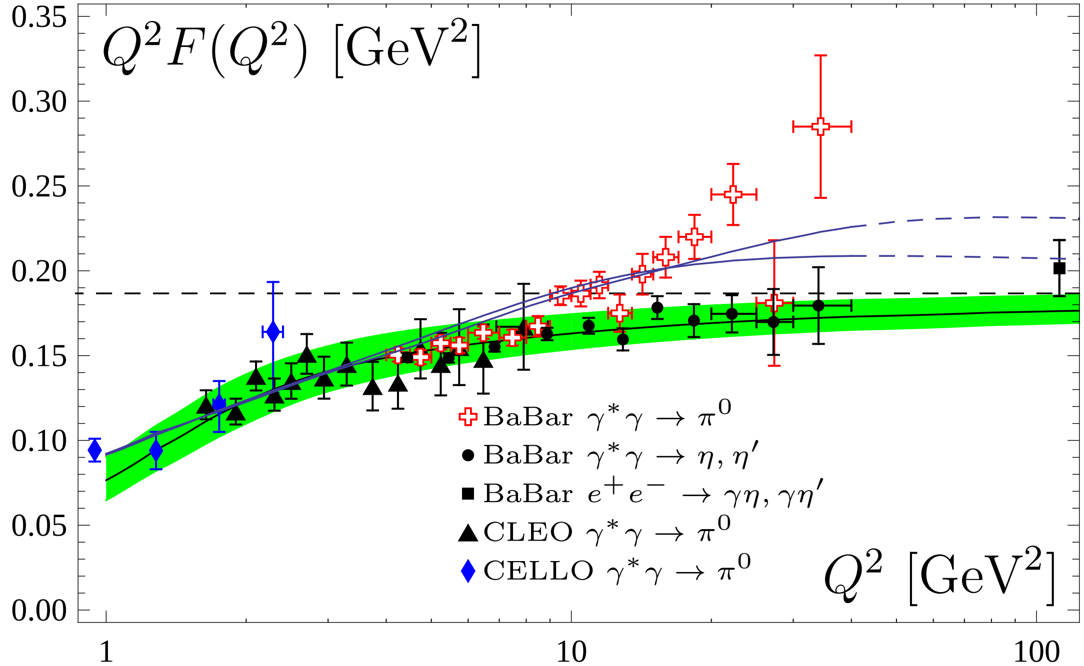

curve	DA
– – – – –	Asymp.QCD
(green band)	BMS bunch
——— Agaev et al	ABOP-1,3 PRD83-054020

- **BMS bunch describes very good all data for $Q^2 \leq 9$ GeV^2.**
- **Note added BaBar $\gamma^*\gamma \to \eta, \eta'$ and $e^+e^- \to \gamma\eta, \gamma\eta'$ data (1101.1142[hep-ex]): All they are inside BMS strip !**
- **ABOP models are in between two sets of BaBar data.**

Inverse Problem:

Fitting Pion DA

from experimental data

—

Confidential Regions

Fitting pion DA under LCSR

- **We fitted experimental data on $\pi\gamma$ TFF by varying Gegenbauer coefficients of Pion DA.**

Fitting pion DA under LCSR

- **We fitted experimental data on $\pi\gamma$ TFF by varying Gegenbauer coefficients of Pion DA.**
- **Two sets of experim. data ($1-9\,\mathrm{GeV}^2$ & 1–40 GeV^2) were analyzed to show the influence of BaBar Data on Pion DA.**

Fitting pion DA under LCSR

- **We fitted experimental data on $\pi\gamma$ TFF by varying Gegenbauer coefficients of Pion DA.**
- **Two sets of experim. data ($1-9$ GeV^2 & 1–40 GeV^2) were analyzed to show the influence of BaBar Data on Pion DA.**

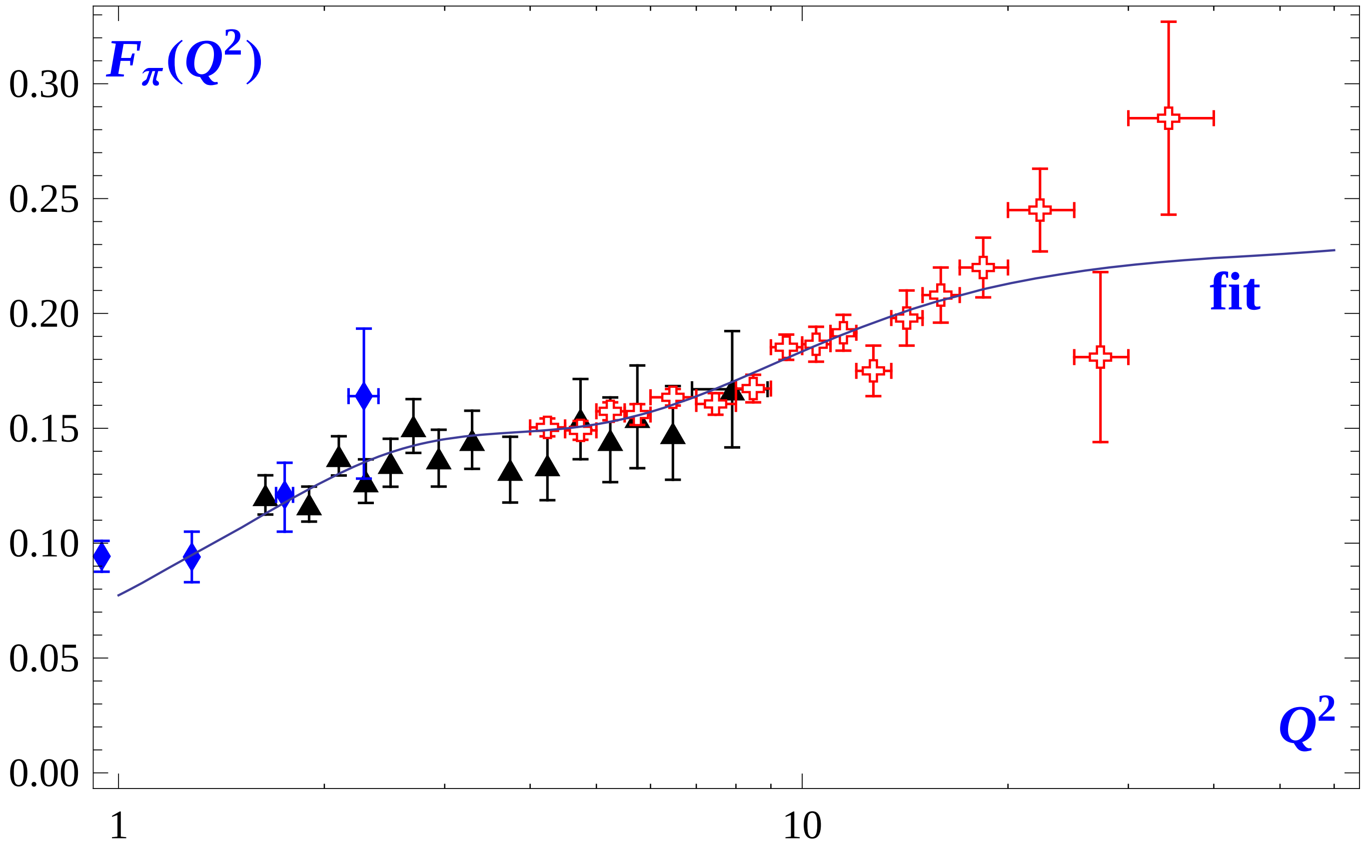

Fit based on LCSRs with NLO+Tw4+3 Gegenbauers

How many harmonics take into account?

The goodness-of-fit χ^2_{ndf}-criterion vs conventional error ($\mathbf{68.3\%}$ CL) as a function on number $\boldsymbol{n}$ of fit parameters

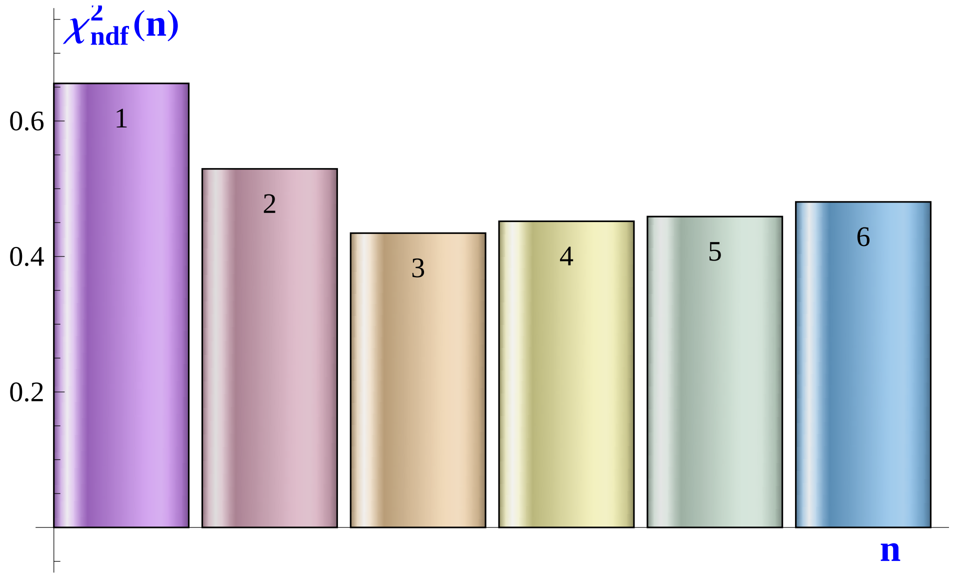

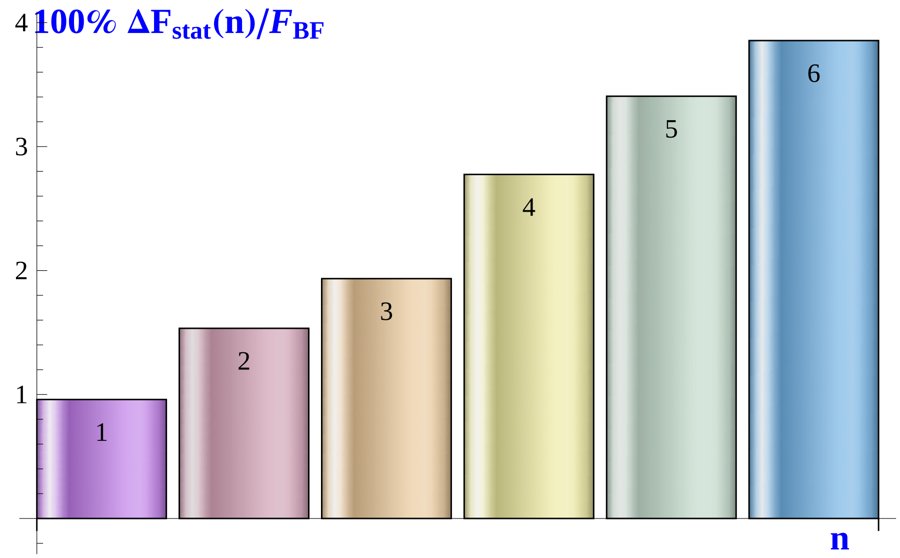

$\mathbf{1-9}$ Gev$^{\mathbf{2}}$ data region

- Goodness - stable, while the error grows with $\boldsymbol{n}$
- The compromise at $\chi^2_{\text{ndf}} \approx \mathbf{0.5}$ and $\boldsymbol{n} = \mathbf{2, 3}$ is enough.

How many harmonics take into account?

The goodness-of-fit χ^2_{ndf}-criterion vs conventional error (68.3% CL) as a function on number n of fit parameters

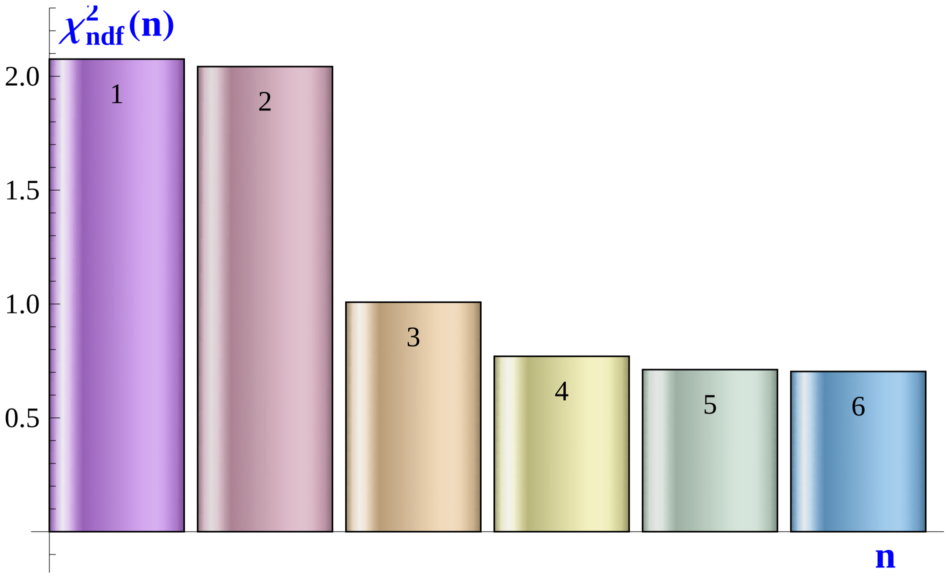

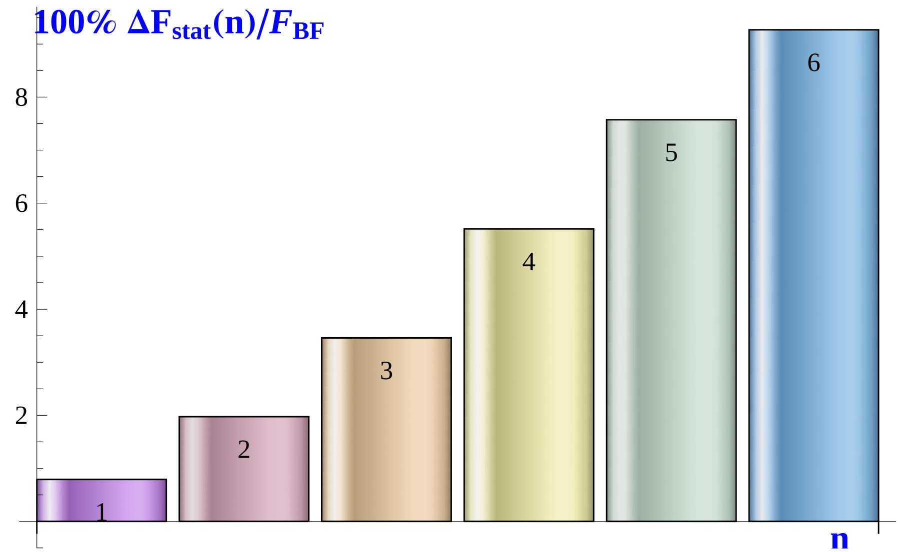

$1-40$ Gev^2 data region

- For fitting $1-40$ Gev^2 data region one should take $n \geq 3$ parameters.

NLC SR Results vs 3D Constraints

BMPS [PRD84(2011)034014]: 3D 1σ-error ellipsoid at $\mu_{\text{SY}} = 2.4$ GeV scale without $\Delta\delta^2_{\text{tw4}}$ uncertainty

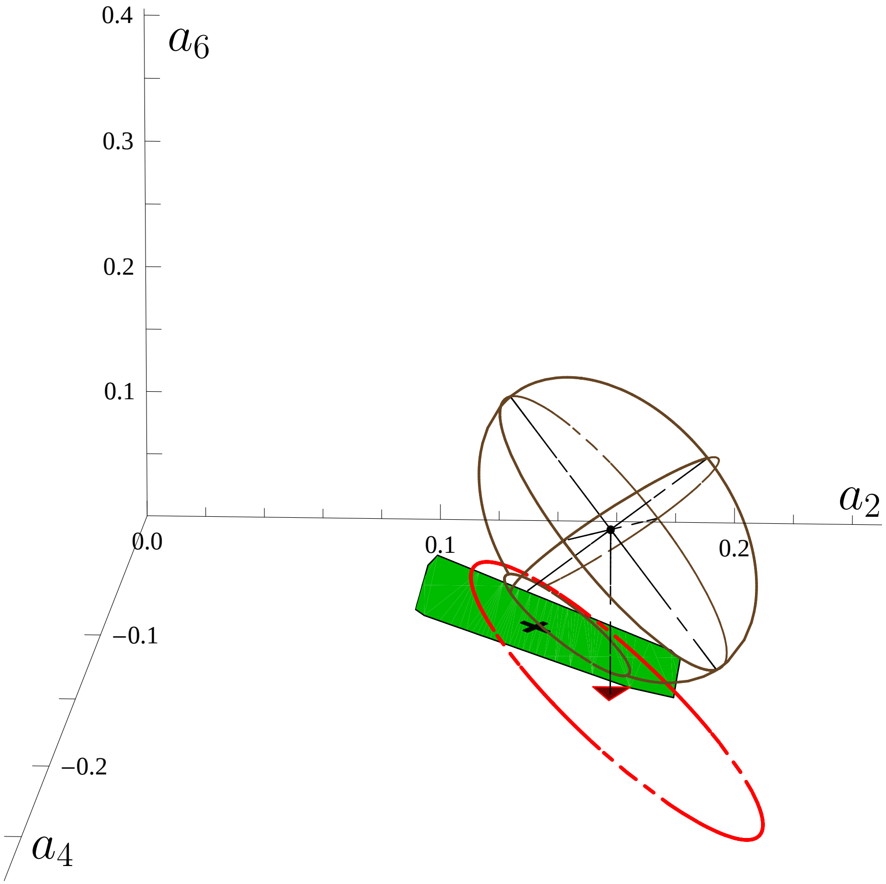

Data Set $1 - 9$ GeV^2

— $\Leftrightarrow$ 2D projection of 1σ-error ellipsoid

▼ $\Leftrightarrow$ $\chi^2_{\text{ndf}} \approx 0.4$

✖ $\Leftrightarrow$ BMS model with $\chi^2_{\text{ndf}} \approx 0.5$

Best-fit $= (0.17, -0.14, 0.12 \pm 0.14)$

BMS $= (0.14, -0.09)$

Good agreement of all data at $Q^2 \leq 9$ GeV^2

At 68.3% CL we have good intersection 2D$\cap$3D$\cap$4D$\neq \emptyset$

NLC SR Results vs 3D Constraints

BMPS [PRD84(2011)034014]: 3D 1σ-error ellipsoid at $\mu_{\text{SY}} = 2.4$ GeV scale without $\Delta\delta^2_{\text{tw4}}$ uncertainty

Data Set $1-9$ GeV^2		
—	$\Leftrightarrow$	2D projection of 1σ-error ellipsoid
▼	$\Leftrightarrow$	$\chi^2_{\text{ndf}} \approx 0.4$
x	$\Leftrightarrow$	BMS model with $\chi^2_{\text{ndf}} \approx 0.5$

Best-fit $= (0.17, -0.14, 0.12 \pm 0.14)$
BMS $= (0.14, -0.09)$

Good agreement of all data at $Q^2 \leq 9$ GeV^2
At 68.3% CL we have good intersection 2D$\cap$3D$\cap$4D$\neq \emptyset$

NLC SR Results *vs* 3D Constraints

BMPS [PRD84(2011)034014]: 3D 1σ-error ellipsoid at $\mu_{\text{SY}} = 2.4$ GeV scale without $\Delta\delta^2_{\text{tw4}}$ uncertainty

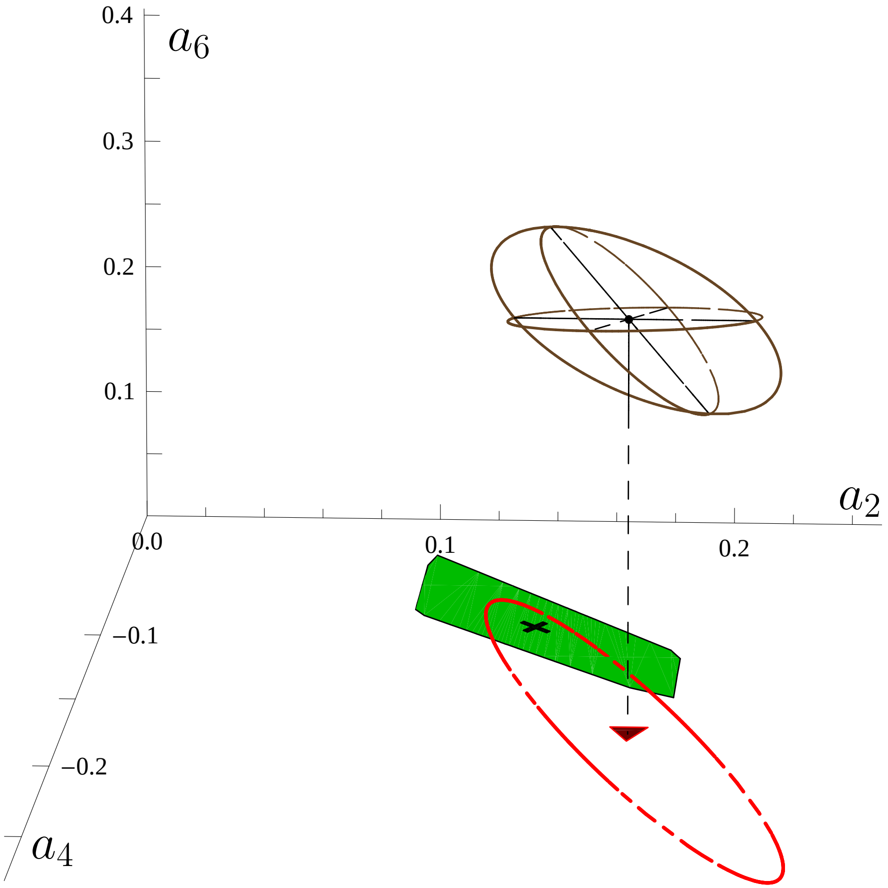

Data Set $1 - 40\,\text{GeV}^2$	
— $\Leftrightarrow$	2D projection of 1σ-error ellipsoid
▼ $\Leftrightarrow$	$\chi^2_{\text{ndf}} \approx 1.0$
x $\Leftrightarrow$	BMS model with $\chi^2_{\text{ndf}} \approx 3.1$

Best-fit $= (0.18, -0.17, 0.31 \pm 0.1)$
BMS $= (0.14, -0.09)$

Bad agreement of all data at $Q^2 \leq 40$ GeV^2
At 68.3% CL we have no intersection 2D∩3D$= \varnothing$, 3D∩4D$= \varnothing$.

NLC SR Results vs 2D Constraints

NLC-bunch and lattice prediction at $\mu_{\text{SY}} = 2.4$ GeV scale with accounting for $\Delta\delta^2_{\text{tw4}}$ uncertainty.

DAs: ◆ ⇔ Asymp., ▲ ⇔ ABOP-3, ✖ ⇔ BMS, ■ ⇔ CZ

Lattice'10 estimate of a_2 are shown by vertical lines.

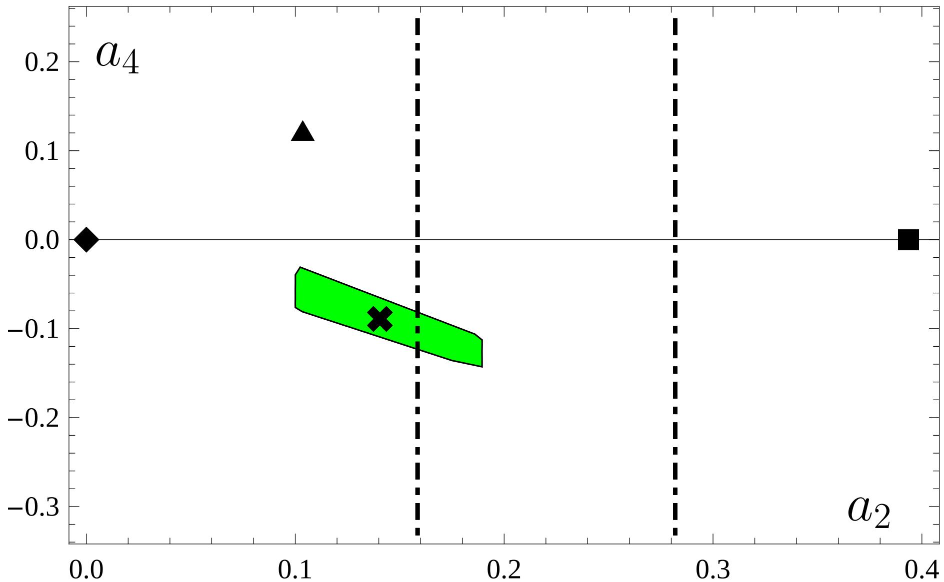

Data Set $1 - 9\,\text{GeV}^2$

BMS bunch agrees well with the lattice data

NLC SR Results vs 2D Constraints

2D-Analysis of the data at $\mu_{\text{SY}} = 2.4$ GeV scale with accounting for $\Delta\delta^2_{\text{tw4}}$ uncertainty.

DAs: ◆ $\Leftrightarrow$ Asymp., ▲ $\Leftrightarrow$ ABOP-3, ✖ $\Leftrightarrow$ BMS, ■ $\Leftrightarrow$ CZ

Lattice'10 estimate of a_2 are shown by vertical lines.

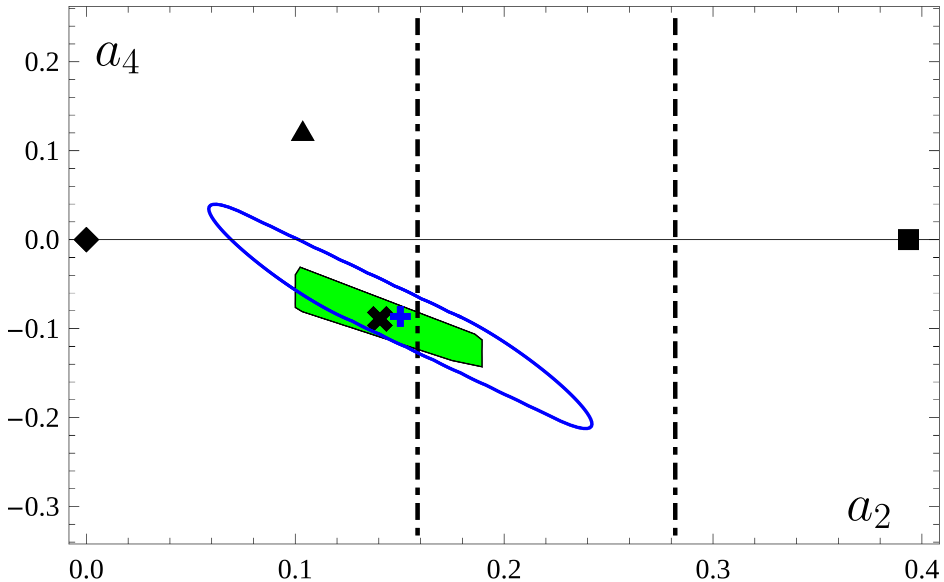

Data Set $1 - 9$ GeV^2

—— $\Leftrightarrow$ **2D 1σ-error ellipse**

BMS bunch agrees well with the lattice data

BMS bunch has better agreement with data up 9 GeV^2 than with CLEO data only.

NLC SR Results vs 2D Constraints

2D-Analysis of the data at $\mu_{\text{SY}} = 2.4$ GeV scale with accounting for $\Delta\delta^2_{\text{tw4}}$ uncertainty.

DAs: ◆ ⇔ Asymp., ▲ ⇔ ABOP-3, ✖ ⇔ BMS, ■ ⇔ CZ

Lattice'10 estimate of a_2 are shown by vertical lines.

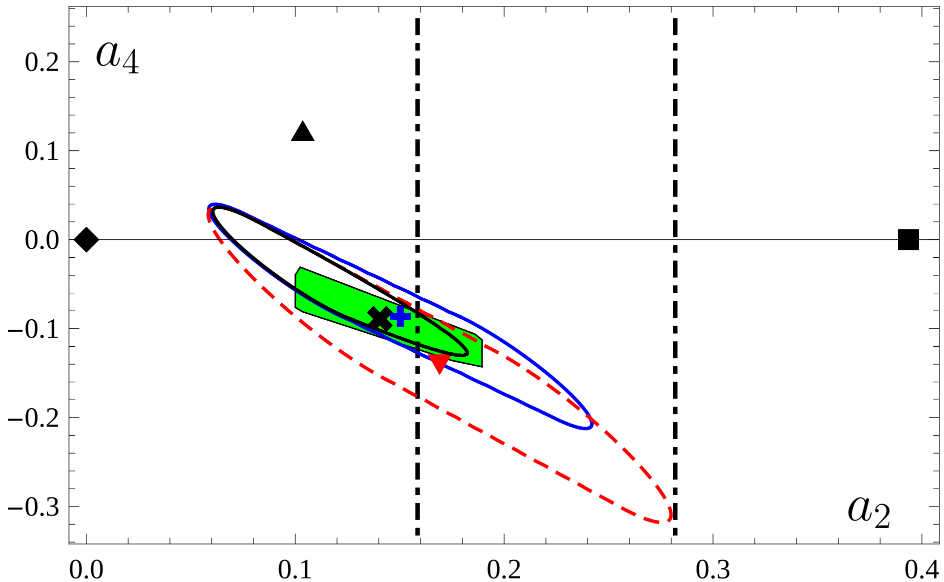

Data Set $1 - 9\,\text{GeV}^2$

- ⇔ 2D 1σ-error ellipse
- ⇔ 2D-Proj. 3D-ellipsoid
- ⇔ $a_6 = 0$ cut of 3D-ellipsoid

BMS bunch agrees well with the lattice data

BMS bunch has better agreement with data up 9 GeV^2 than with CLEO data only.

NLC SR Results vs 2D Constraints

BMPS [arXiv:1105.2753 [hep-ph]]: 2D 1σ-error ellipses at $\mu_{\text{SY}} = 2.4$ GeV scale with accounting for $\Delta\delta^2_{\text{tw4}}$ uncertainty.

DAs: ◆ ⇔ Asymp., ▲ ⇔ ABOP-3, ✖ ⇔ BMS, ■ ⇔ CZ

Lattice'10 estimate of a_2 are shown by vertical lines.

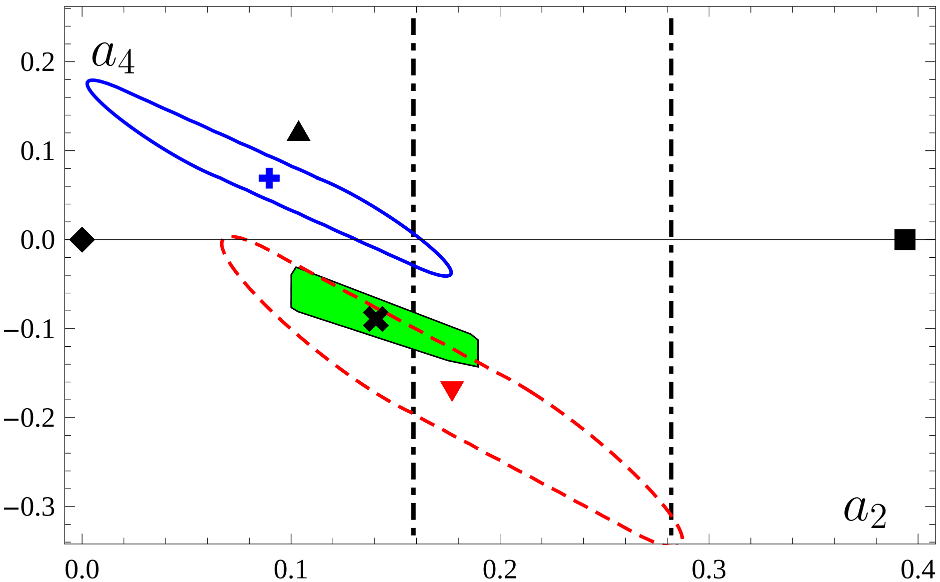

Data Set $1 - 40\,\text{GeV}^2$
—— ⇔ 2D 1σ-error ellipse
- - - ⇔ 2D-Proj. 3D-ellipsoid

Bad agreement with 2D 1σ-error ellipse

No cross-section with $a_6 = 0$ plane.

3D Data Fit of Pion DA vs BMS (QCD SR)

:= BMS, **:= $1-9\,\text{GeV}^2$**, **:= $1-40\,\text{GeV}^2$**

at $\mu_{\text{SY}} = 2.4\,\text{GeV}$ scale.

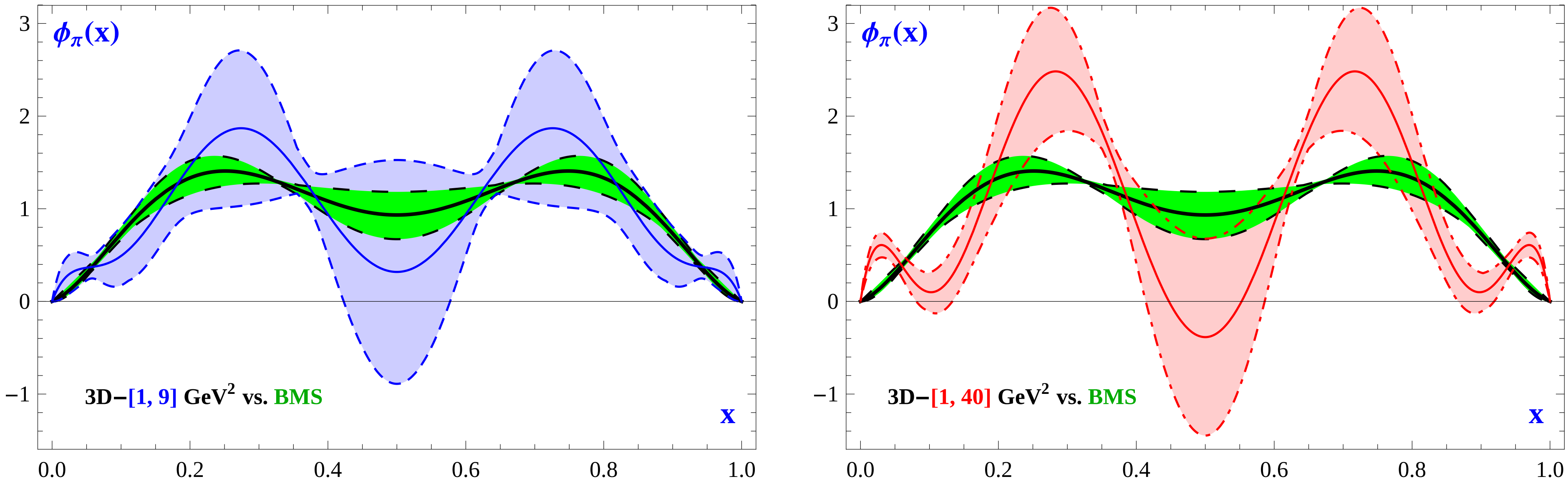

- **BMS bunch agrees well with Data Set $1-9\,\text{GeV}^2$;**

3D Data Fit of Pion DA vs BMS (QCD SR)

$:=$ BMS, $:= 1 - 9\,\mathbf{GeV}^2$, $:= 1 - 40\,\mathbf{GeV}^2$

at $\mu_{\mathsf{SY}} = 2.4\,\mathbf{GeV}$ scale.

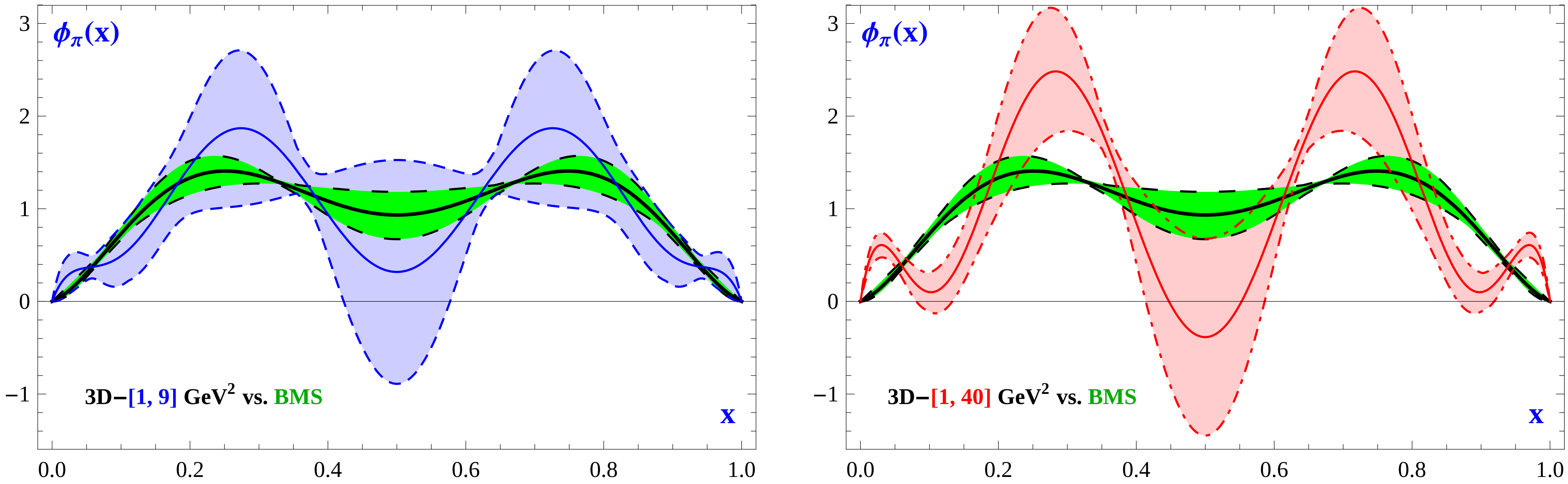

- **BMS bunch** agrees well with Data Set $1 - 9\,\mathbf{GeV}^2$;
- **New BaBar Data** do not agree with **BMS bunch** based on **NLC QCD SRs**.

3D Data Fit of Pion DA vs BMS (QCD SR)

$:=$ BMS, $:= 1-9\,\text{GeV}^2$, $:= 1-40\,\text{GeV}^2$

at $\mu_{\text{SY}} = 2.4\,\text{GeV}$ scale.

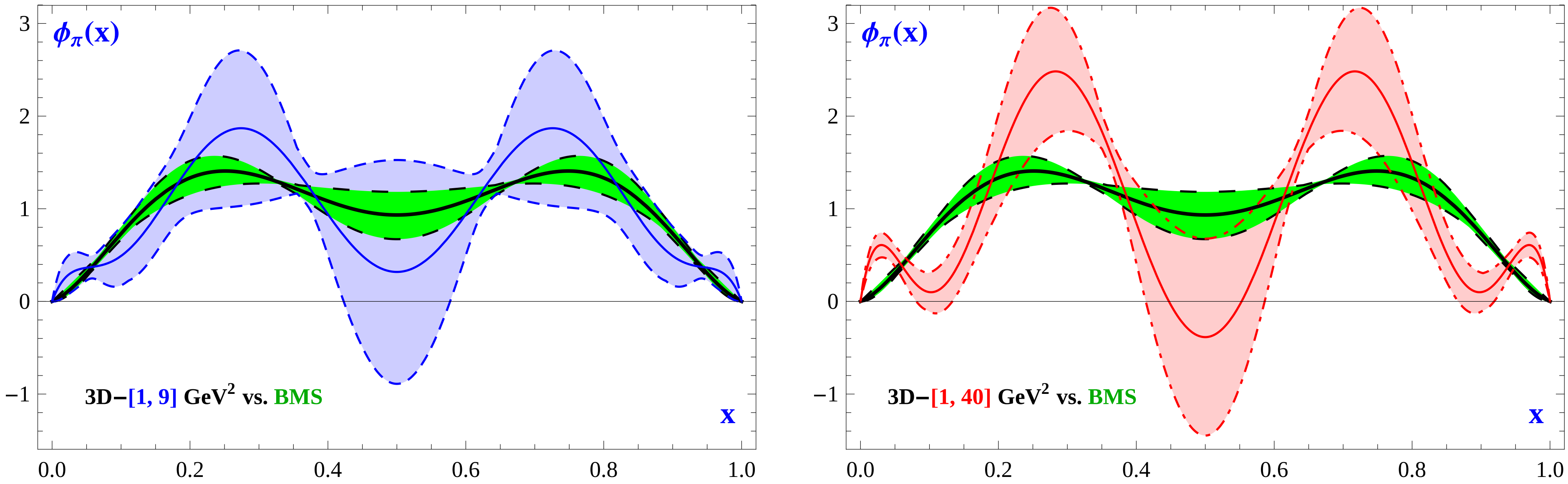

- **BMS bunch** agrees well with Data Set $1-9\,\text{GeV}^2$;
- **New BaBar Data** do not agree with **BMS bunch** based on **NLC QCD SRs**.
- Both data sets does not match each other.

End-point Bechavior of Pion DA

Integral derivative $D^{(2)}\varphi(x) = \frac{1}{x}\int_0^x \frac{\varphi(y)}{y} dy$

is an average derivative $\varphi'_\pi(x)$ **near the end-point** $x = 0$**.**

Important property: $\lim\limits_{x\longrightarrow 0} D^{(2)}\varphi(x) = \varphi'_\pi(0)$**.**

End-point Bechavior of Pion DA

Integral derivative $D^{(2)}\varphi(x) = \frac{1}{x}\int_0^x \frac{\varphi(y)}{y}dy$

at $\mu_{\text{SY}} = 2.4$ GeV scale.

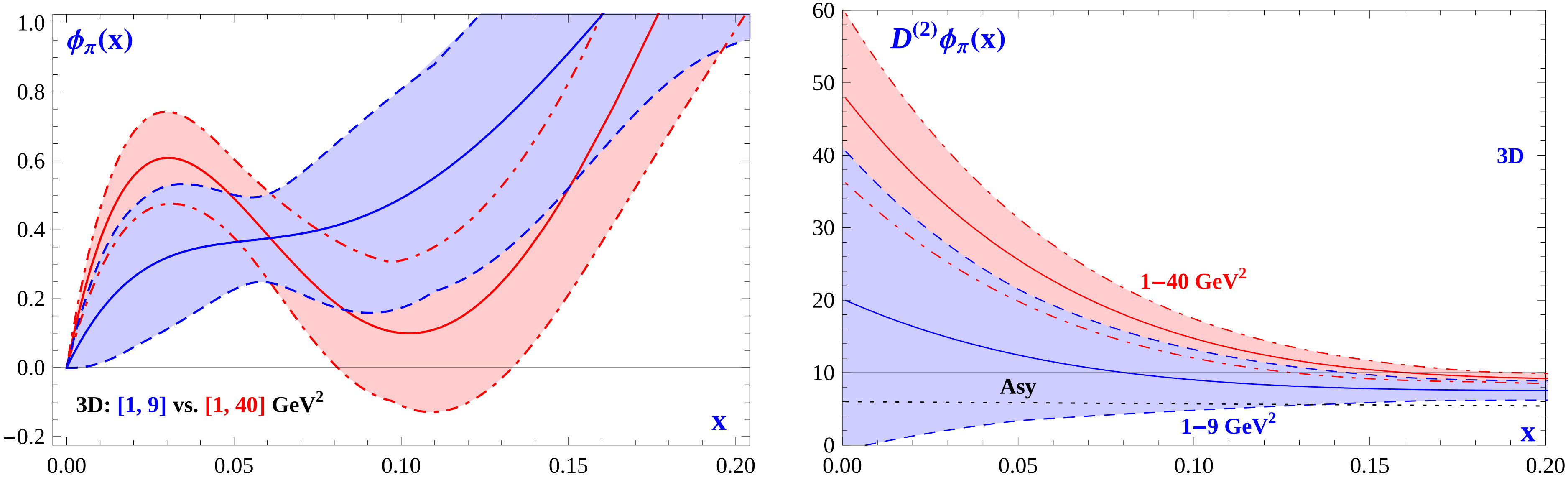

- **DA**$^{1-9\ \text{GeV}^2}$ **and DA**$^{1-40\ \text{GeV}^2}$ **are separated near the origin.**
- **BaBar Data demands End-Point Enhanced Pion DA.**

Confidential Region for Pion DA Moments vs. Lattice QCD

2D Constraints and Lattice QCD

1σ **region in** $(\langle\xi^2\rangle_\pi, \langle\xi^4\rangle_\pi)$ **plane from 2D**$(1-9$ **GeV**$^2)$ **analysis vs QCDSF&UKQCD Lattice Data [PRD74(2006)074501] at** $\mu_{\text{lat}} = 2$ **GeV scale:**

curve	meaning
———	**2D-**1σ**-ellipse**
– – – – –	**Lattice'06**

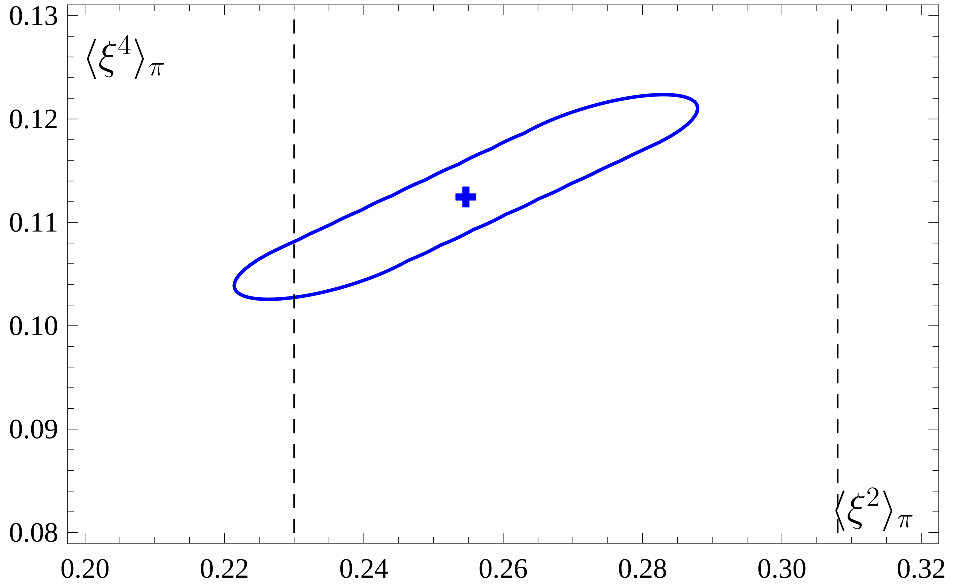

Our 2D-1σ **region is almost completely inside Lattice'06 constraint.**

2D Constraints and Lattice QCD

1σ **region in** $(\langle\xi^2\rangle_\pi, \langle\xi^4\rangle_\pi)$ **plane from 2D**$(1-9$ **GeV**$^2)$ **analysis vs RBC&UKQCD Lattice Data [PRD83(2011)074505] at** $\mu_{\text{lat}} = 2$ **GeV scale:**

curve	meaning
——— (solid)	**2D-1σ-ellipse**
– – – – –	**Lattice'06**
–·–·–·–	**Lattice'10**

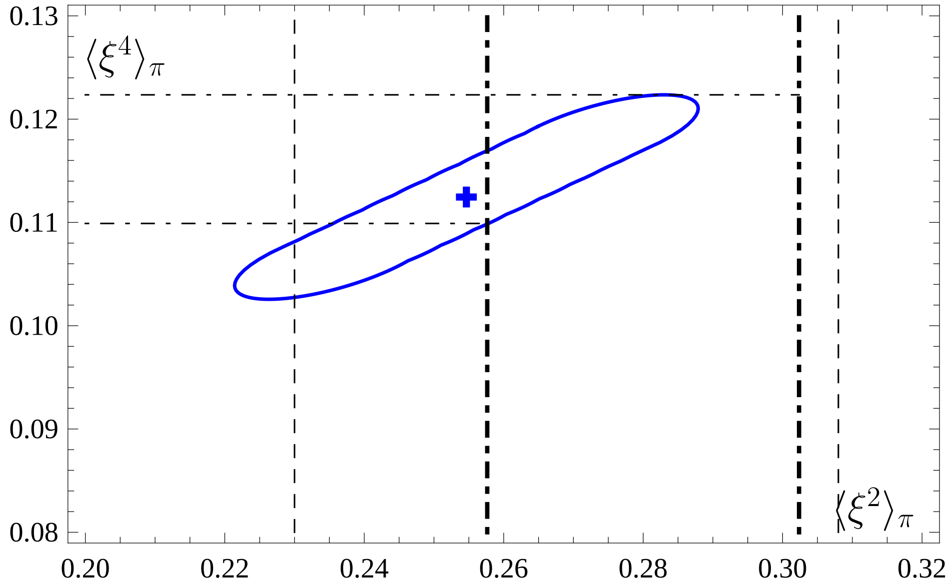

Our 2D-1σ region is one-half inside Lattice'10 constraint.

2D Constraints and Lattice QCD

1σ region in $(\langle\xi^2\rangle_\pi, \langle\xi^4\rangle_\pi)$ plane from 2D$(1-9$ GeV$^2)$ analysis vs RBC&UKQCD Lattice Data [PRD83(2011)074505] at $\mu_{\text{lat}} = 2$ GeV scale:

curve	meaning
———	2D$^{0.7}$-1σ-ellipse
– – – – –	Lattice'06
–·–·–·–	Lattice'10
– – – – –	2D$^{1.5}$-1σ-ellipse

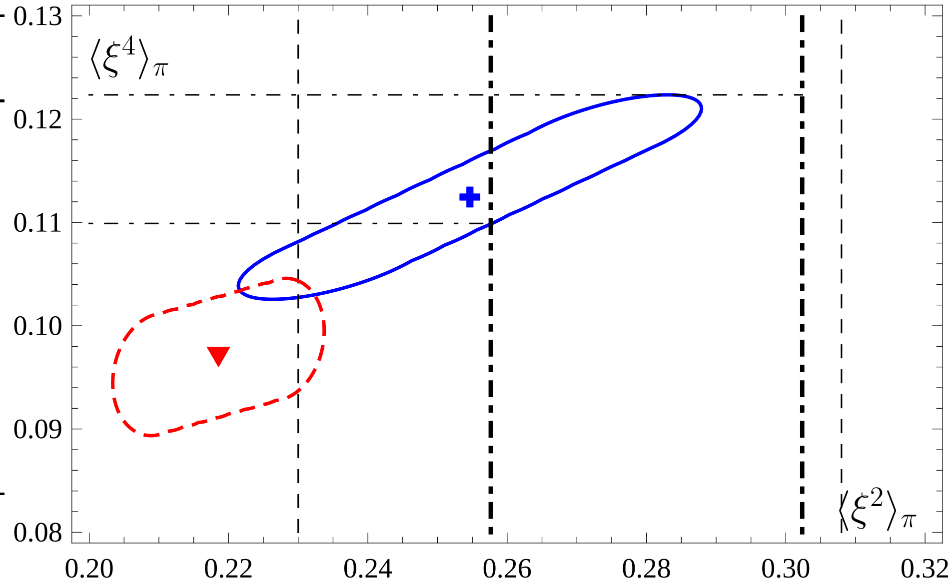

Our 2D-1σ region with $(M^2 \approx 0.7\,$GeV$^2)$ is one-half inside Lattice'10 constraint,

whereas the 2D-1σ region with ABOP value $(M^2 = 1.5$ GeV$^2)$ is completely out of Lattice'10 constraint!

2D Constraints and Lattice QCD

1σ region in $(\langle\xi^2\rangle_\pi, \langle\xi^4\rangle_\pi)$ plane from 2D$(1-9$ GeV$^2)$ analysis vs RBC&UKQCD Lattice Data [PRD83(2011)074505] at $\mu_{\text{lat}} = 2$ GeV scale:

curve	meaning
solid blue line	2D-1σ-ellipse
dashed line	Lattice'06
dash-dotted line	Lattice'10

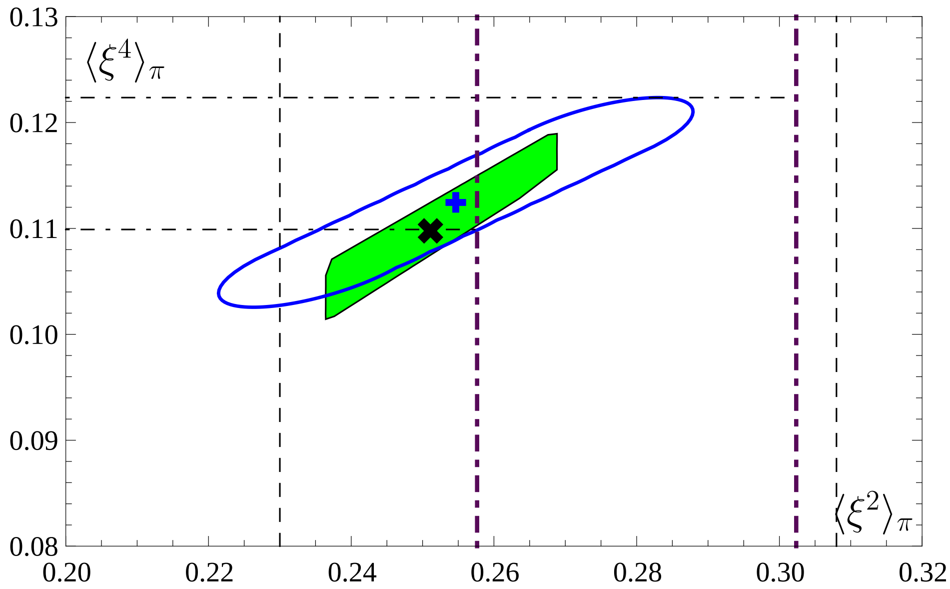

Intersection of Lattice and 2D-1σ region leads to prediction:

$\langle\xi^4\rangle_\pi \in [0.11, 0.122]$ — in a good agreement with estimation $\langle\xi^4\rangle_\pi \in [0.095, 0.134]$ in [Stefanis, NPB.PS.181(2008)199].

Fit Results and Pion DA Models

Comparing Fit Results with Pion DA models

Model/Fit	Values of a_n	χ^2/ndf $(1-9\,\text{GeV}^2)$	χ^2/ndf $(1-40\,\text{GeV}^2)$
a_2, a_4, a_6 Fit	$(0.18, -0.17, 0.31)$	0.4	1.0
BMS	$(0.14, -0.09)$	0.5	3.1
Agaev et al	$(0.08, 0.14, 0.09)$	2.8	2.4
Kroll	$(0.21, 0.01)$	3.8	4.4
AdS/QCD	$0.15, 0.06, 0.03$	2.3	2.8
CZ	(0.39)	32.3	25.5
Asympt.	$(0, 0)$	4.7	7.9

All values given at $\mu_{\text{SY}} = 2.4$ GeV scale.

- **BMS DA** gives best LCSR Description of $\pi\gamma$TFF for $Q^2 \leq 9\,\text{GeV}^2$.
- All-Data LCSR-Fit Result is far from All Considered Pion DA Models.

Comparing Different Data Set Analyses

Q^2 regions	$[1-9]$ GeV^2	$[1-40]$ GeV^2
BMS bunch	Agreement	No!
η and η'	Agreement	No!
Number of harmonics n	$2, 3$	$3, 4$
Best χ^2_{ndf}	$0.53, \; 0.44$	$1.0, \; 0.77$
Derivative $\varphi_\pi(x)\|_{x=0}$	$20.2 \pm 19.8 \pm 1.1$	$48.5 \pm 11.4 \pm 0.4$
Derivative $D^{(2)}\varphi_\pi(0.4)$	$6.6 \pm 1.1 \pm 0.4$	$8.1 \pm 0.7 \pm 0.3$

Conclusions

- **By fitting $\pi\gamma$Transition FF Data in LCSR Approach we obtained Confidential Regions for Gegenbauer coefficients, Moments, and Derivatives of Pion DA.**

Conclusions

- By fitting $\pi\gamma$Transition FF Data in LCSR Approach we obtained Confidential Regions for Gegenbauer coefficients, Moments, and Derivatives of Pion DA.
- Result of fitting the CELLO, CLEO, and BaBar Data up to $9\,\text{GeV}^2$ is in a good agreement with previous CLEO-based fit and prefers the End-Point Suppressed (BMS) Pion DA.

Conclusions

- By fitting $\pi\gamma$Transition FF Data in LCSR Approach we obtained Confidential Regions for Gegenbauer coefficients, Moments, and Derivatives of Pion DA.
- Result of fitting the CELLO, CLEO, and BaBar Data up to $9\,\mathrm{GeV}^2$ is in a good agreement with previous CLEO-based fit and prefers the End-Point Suppressed (BMS) Pion DA.
- Taking into account all the data on $F_{\gamma^*\gamma\to\pi}(Q^2)$, including the new BaBar points with $Q^2 = 10 - 40\,\mathrm{GeV}^2$, requires sizeable coefficient a_6, while a_2 and a_4 remain the same. All-Data-Fit prefers End-Point Enhanced Pion DA.

Conclusions

- By fitting $\pi\gamma$ Transition FF Data in LCSR Approach we obtained Confidential Regions for Gegenbauer coefficients, Moments, and Derivatives of Pion DA.
- Result of fitting the CELLO, CLEO, and BaBar Data up to $9\,\textbf{GeV}^2$ is in a good agreement with previous CLEO-based fit and prefers the End-Point Suppressed (BMS) Pion DA.
- Taking into account all the data on $F_{\gamma^*\gamma\to\pi}(Q^2)$, including the new BaBar points with $Q^2 = 10 - 40\,\textbf{GeV}^2$, requires sizeable coefficient a_6, while a_2 and a_4 remain the same. All-Data-Fit prefers End-Point Enhanced Pion DA.
- Evident conflict between ($\eta\gamma$ and $\eta'\gamma$) and $\pi^0\gamma$ BaBar Data may signal about strong isospin symmetry violation in pseudoscalar meson sector.

Conclusions

- By fitting $\pi\gamma$Transition FF Data in LCSR Approach we obtained Confidential Regions for Gegenbauer coefficients, Moments, and Derivatives of Pion DA.
- Result of fitting the CELLO, CLEO, and BaBar Data up to $9\,\text{GeV}^2$ is in a good agreement with previous CLEO-based fit and prefers the End-Point Suppressed (BMS) Pion DA.
- Taking into account all the data on $F_{\gamma^*\gamma\to\pi}(Q^2)$, including the new BaBar points with $Q^2 = 10 - 40\,\text{GeV}^2$, requires sizeable coefficient a_6, while a_2 and a_4 remain the same. All-Data-Fit prefers End-Point Enhanced Pion DA.
- Evident conflict between ($\eta\gamma$ and $\eta'\gamma$) and $\pi^0\gamma$ BaBar Data may signal about strong isospin symmetry violation in pseudoscalar meson sector.
- To resolve BaBar puzzle we need Belle verification of $\pi\gamma$Transition FF Data.

"Twist-6" contribution [Agaev et al, PRD83,0540020(2011)]

$$\rho^{(t=6)}(Q^2,x) \;=\; 8\pi C_F\alpha_s(\mu)\frac{\langle\bar{q}q\rangle^2}{N_c f_\pi^2}\frac{x^2}{Q^6}\left[2x\log x + 2x\log\bar{x} - x + 2\delta(\bar{x}) - \left[\frac{1}{1-x}\right]_+\right].$$

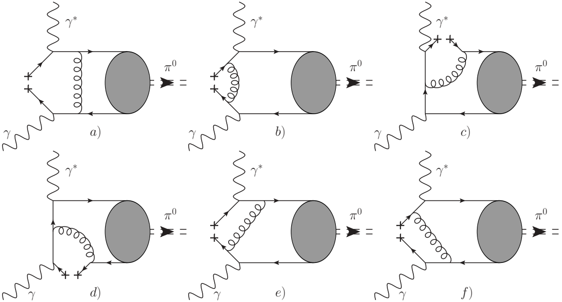

$$\rho^{(t=6)}(Q^2,x) \sim 8\pi C_F\alpha_s(\mu)\frac{\langle\bar{q}q\rangle^2}{Q^6}$$

express the inverse power correction to coefficient function rather than the geometric twist-6

BaBar Doubts about BaBar data?

- BaBar Collaboration also measured FFs of $\gamma^*\gamma \to \eta$ and $\gamma^*\gamma \to \eta'$, see [Arxiv:1101.1142].
- From η and η' FFs they extracted hypothetical n FF using $\eta - \eta'$ mixing in the quark flavor basis:

$$|n\rangle = \frac{1}{\sqrt{2}}(|\bar{u}u\rangle + |\bar{d}d\rangle), \qquad |s\rangle = |\bar{s}s\rangle,$$

$$|\eta\rangle = \cos\phi\,|n\rangle - \sin\phi\,|s\rangle, \qquad |\eta'\rangle = \sin\phi\,|n\rangle + \cos\phi\,|s\rangle,$$

with $\phi = 39.9^\circ \pm 2.9^\circ$.

- Take into account flavor structure and quark charges $\Rightarrow$ $e_u^2 + e_d^2 = \frac{5}{3} \cdot (e_u^2 - e_d^2) \Rightarrow$ factor $\frac{5}{3}$.

BaBar Doubts about BaBar data?

- **BaBar Collaboration also measured FFs of $\gamma^*\gamma \to \eta$ and $\gamma^*\gamma \to \eta'$, see [Arxiv:1101.1142].**

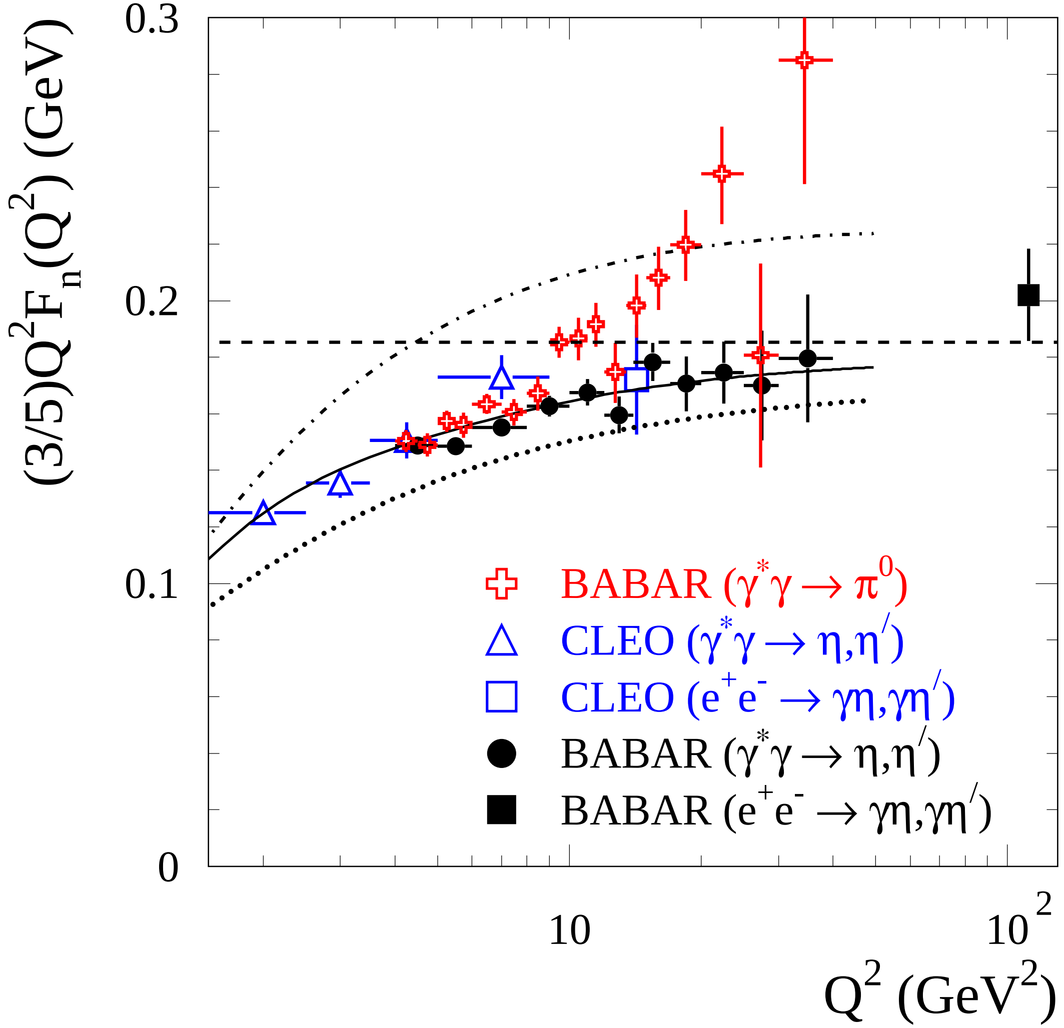

curve	πDA
dash-dotted	CZ
solid	BMS
dotted	Asymp.

BMS-curve goes just through the new BaBar data!

$\gamma^*\gamma \to \pi^0$ BaBar data are in contradiction with $\gamma^*\gamma \to \eta, \eta'$ BaBar data!

Attempts to solve the “pion puzzle”

A possible scenarios to explain the BaBar data

- **A. Dorokhov [0905.3577] with constituent quark model**

$Q^2\, F_{\gamma^*\gamma\to\pi}(Q^2) \sim \ln^2(Q^2/M_q^2)$ **with** $M_q \simeq 135$ **MeV.**

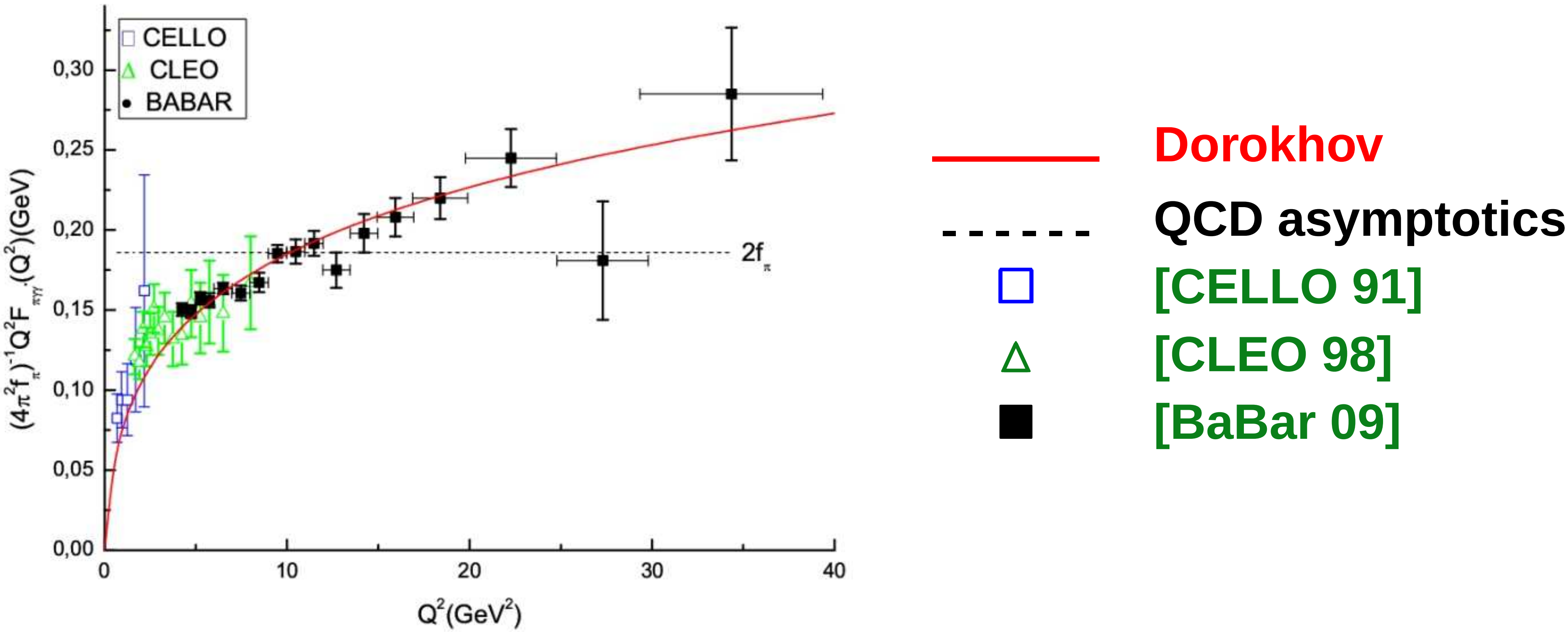

Note $M_q \simeq 135$ **MeV** $<$ 300 **MeV. No trace of QCD...**

Attempts to solve the "pion puzzle"

A possible scenarios to explain the BaBar data

- **A. Radyushkin [0906.0323] with "flat" DA $\varphi_\pi(x) \approx 1$ and using Light-Front Gaussian model:**

$$Q^2\, F^{\text{LFG}}_{\gamma^*\gamma\to\pi}(Q^2) \sim \int\limits_0^1 \frac{\varphi_\pi(x)}{x}\left[1 - \textbf{exp}\left(-\frac{x\, Q^2}{2\,\bar{x}\,\sigma}\right)\right] dx$$

Here $\sigma \simeq 0.53$ GeV^2.

Attempts to solve the “pion puzzle”

A possible scenarios to explain the BaBar data

- **A. Radyushkin [0906.0323] with “flat” DA $\varphi_\pi(x) \approx 1$:**

$$Q^2\, F^{\mathsf{LFG}}_{\gamma^*\gamma\to\pi}(Q^2,0) \sim \ln\left[\frac{Q^2}{M^2}\right], \quad M^2 = 2\sigma e^{-\gamma_E} \simeq 0.6\ \mathsf{GeV}^2.$$

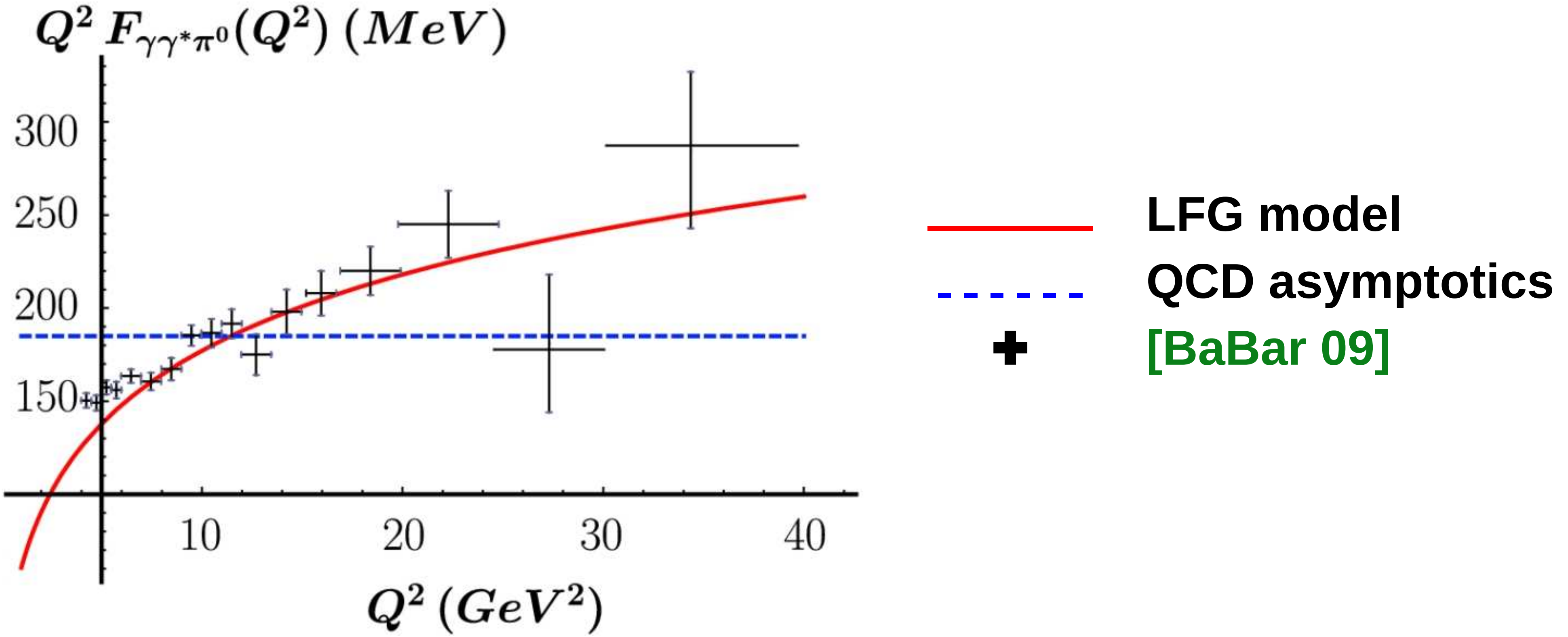

No Factorization. Rad. Corrs. removed by hand!

Attempts to solve the "pion puzzle"

A possible scenarios to explain the BaBar data

- **M. Polyakov [0906.0538] with "flat" DA**

$\varphi_\pi(x, \mu_0 = 0.6\ \text{GeV}) = 1.3 - 0.3 \cdot 6\, x\, (1 - x)$ **and using:**

$$Q^2\, F^{\text{Pol}}_{\gamma^*\gamma\to\pi}(Q^2) \sim \int_0^1 \frac{\varphi_\pi(x, Q^2)}{x + m^2/Q^2}\, dx$$

Here $m \simeq 0.65\ \text{GeV}$ **from BaBar data fit.**

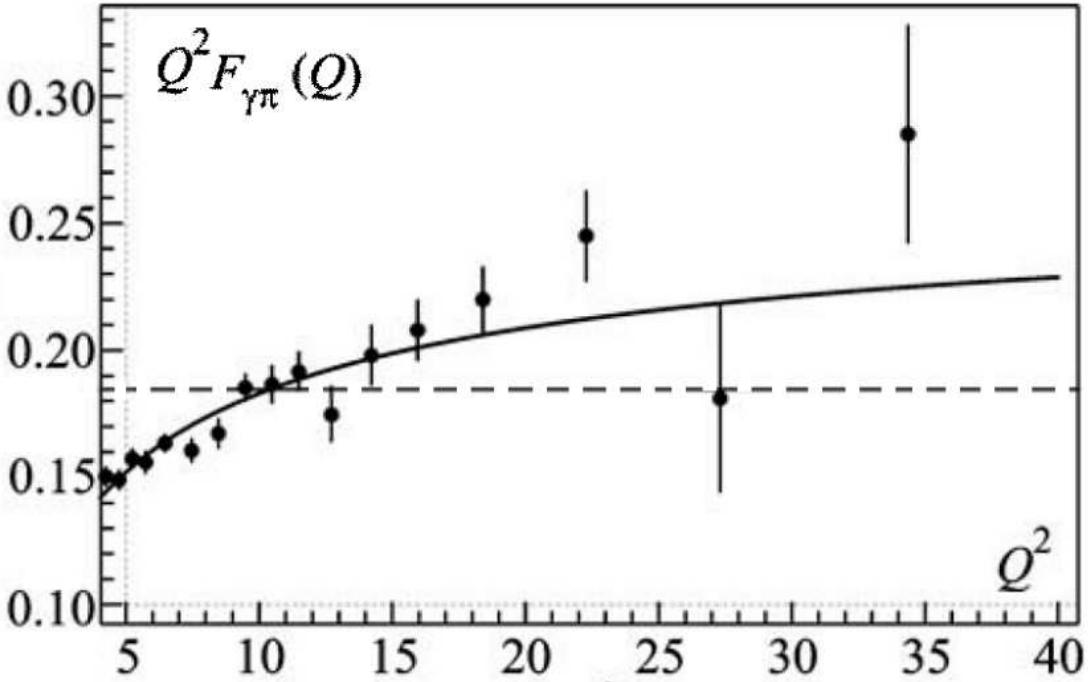

Polyakov
QCD asymptotics
[BaBar 09]

QCD Evolution is here!